OUKA
The University of Osaka
Institutional Knowledge Archive

Title	STRUCTURAL STUDIES ON BLUE COPPER PROTEINS
Author(s)	井上, 豪
Citation	大阪大学, 1994, 博士論文
Version Type	VoR
URL	https://doi.org/10.11501/3094148
rights	
Note	

The University of Osaka Institutional Knowledge Archive : OUKA

https://ir.library.osaka-u.ac.jp/

The University of Osaka

STRUCTURAL STUDIES ON BLUE COPPER PROTEINS

TSUYOSHI INOUE

OSAKA UNIVERSITY

1994

STRUCTURAL STUDIES ON BLUE COPPER PROTEINS

(ブルー銅蛋白質に関する構造学的研究)

TSUYOSHI INOUE

OSAKA UNIVERSITY

1993

Preface

The work presented in this thesis has been performed under the guidance of Professor Yoshiki Ohshiro at the Department of Applied Chemistry, Faculty of Engineering Osaka University.

Tsuyoshi Inoue

Department of Applied Chemistry
Faculty of Engineering
Osaka University
Yamadaoka 2-1, Suita,
Osaka 565,
Japan

January, 1994

Contents

Abbreviations

PAZAM1	pseudoazurin from *methylobacterium extorquens* AM1
PAZIAM	pseudoazurin from *achromobacter cycloclastes* IAM1013
AZUNCIB	azurin from *achromobacter xylosoxidans* NCIB11015
PCYSIL	plastocyanin from *silene*
MR	molecular replacement
MAD	multiwavelength anomalous dispersion
EPR	electron paramagnetic resonance
PAZS6	pseudoazurin from *alcaligenes faecalis* S-6
AZUNCTC	azurin from *alcaligenes denitrificans* NCTC8582
AZUAER	azurin from *pseudomonas aeruginosa*
MADH	methylamine dehydrogenase
SAS	saturated-ammonium sulfate
NIR	nitrite reductase
IP	imaging plate
MIR	multiple isomorphous replacement
SIR	single isomorphous replacement
r.m.s	root mean square
PCY	plastocyanin from *poplar*

1 Introduction

Copper atom that is tracely contained, but required for biological system, has important roles such as electron transfer, oxidation-reduction catalyst, transportation of oxygen, preservation of copper, and so on. Because the blue copper proteins concerning electron transportation have very beautiful blue color and have widely distributed from bacteria to high plants, many bioinorganists have been interested in the distinctive color and functions. So far the studies on the relationships between molecular structures and their functions of blue copper proteins have been actively performed and four molecular structures of the typical blue copper proteins have been revealed by X-ray crystallography. The first is plastocyanin from *poplar* that is analyzed by Freeman (Freeman, 1978) and the others are two azurins (Baker, E. N. 1988, Adman, E. T., 1978), one pseudoazurin (Adman, 1989) and one amicyanin (Chen, L. *et al.*, 1993). Those crystal structures revealed that the three-dimensional structure of each blue copper protein was basically constructed by a β–barrel that was formed by eight β-strands and the location of copper was commonly at the northern end of the molecule. It was also common to all blue copper proteins except stellacyanin that the active site structures around the copper atoms were formed by four

conserved amino acids (two histidine, one cysteine and one methionine). Although the active sites of the typical blue copper proteins had been revealed, it was partially unclear that the relationship between their three-dimensional structures and their characteristic functions, such as the properties of the visible absorbance, EPR spectrum, high reduction potential and electron-transportation and so on.

Many copper complexes imitating the active sites in the blue copper proteins have been synthesized to put them to practical use, but it is so difficult to make use of a complex for practical application as well as to synthesize a copper complex with characteristic functions like blue copper proteins.

With these backgrounds, in order to make clear the relationships between the three-dimensional structures and the characteristic functions and to establish the structural principle for synthesizing a copper complex with the distinctive functions in the blue copper proteins, I tried X-ray crystallographic studies on four blue copper proteins. One is pseudoazurin from *methylobacterium extorquens* AM1 (PAZAM1), another is pseudoazurin from *achromobacter cycloclastes* IAM1013 (PAZIAM), another is azurin from *achromobacter xylosoxidans* NCIB11015 (AZUNCIB) and the other is plastocyanin from high plant of *Silene* (PCYSIL). I have

In this work the detail comparison among the structures of typical blue copper proteins has also revealed the relationships between the structures and the functions, especially the subtle differences of the visible absorption spectrum and EPR spectrum in the blue copper proteins.

I report the results of the X-ray structure analysis and the structural principles of three blue copper proteins besides the details of the molecular structures. Those are to contain some structural principles for designing a copper complex with the characteristic properties in blue copper proteins.

1-1 Properties and Classification of Copper Proteins

While a large amount of 11 kinds of elements are found in biological system, 17 are contained in extremely little amount. Copper that is following iron and zinc is the third most in biological atmosphere and have many important roles (Fig. 1-1).

Fig. 1-2 shows the properties and functions of copper proteins. When copper atoms are contained as ions in proteins, they have many roles, such as electron transport, oxidation-reduction catalyst, transportation of oxygen, preservation of copper, and so on. These copper proteins are classified in three groups. A type-1 copper ion is possible to assigned by EPR spectrum and colored in blue. In contrast to that a type-2 copper atom is in non-blue. Since a type-3 copper ion exists as binuclear, it is indetectable by EPR spectrum (Table 1-1). Among them Type-1 copper proteins have attractive blue color that they are called as blue copper proteins.

1-2 Properties of Blue Copper Proteins

Blue copper proteins studied in this work contain a type-1 copper ion in each protein and concern the electron transport chain.

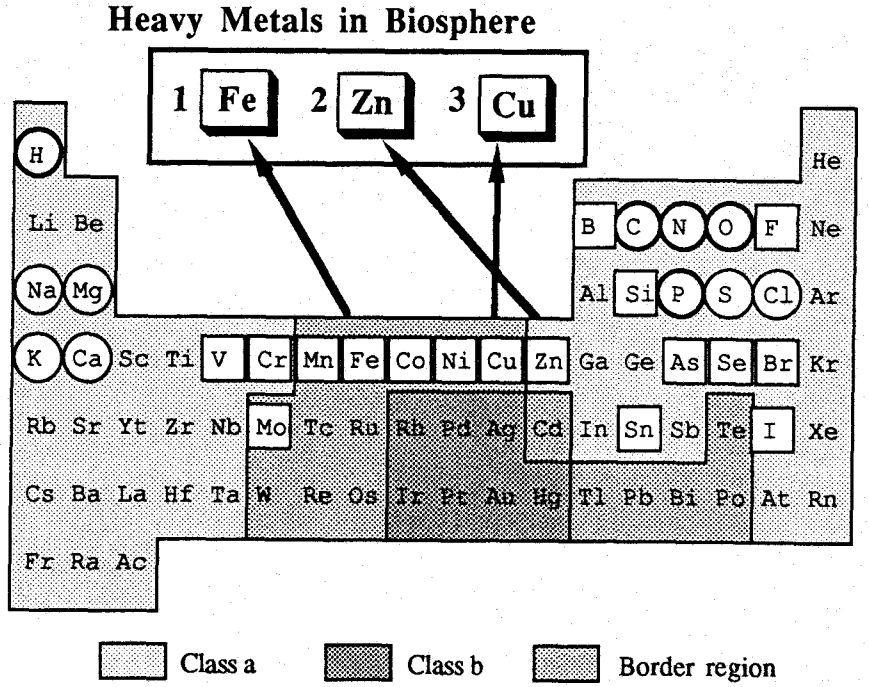

Elemental Composition (Human)

O	62.8×10^4 (ppm)	Fe	50 (ppm)
C	19.4×10^4	Zn	25
H	9.3×10^4	Cu	4
N	5.1×10^4		

The roles of Metal ions

1. Maintance of structure (K, Ca, Mg, Mn)
2. Signal control (Na, K, Mg, Ca)
3. Reaction in vivo. (Mg, Ca, Mn, Zn)
4. Oxidation & Reduction (**Cu, Fe, Co, Mo**)

Fig. 1-1. Essential bioelements are shown in the periodic chart. While a great deal of 11 elements (signed by circles) are contained, a small quanity of 17 (shown by squares) are in the biological system

Table 1-1 *Properties and Functions of Copper Proteins*

Functions of Copper Proteins

(1) Electron Transfer
ex. azurin, pseudoazurin, plastocyanin, rusticyanin, stellacyanin, umecyanin, mavicyanin, plantacyanin

(2) Oxidation-Reduction Catalyst
ex. quercetinase, tyrosinase, dopamine-b-hydroxylase, galactose oxidase, laccase, ceruloplasmin, amine oxidase, nitrite reductase, ascorbate oxidase, indole 2, 3-dioxygenase, superoxide dismutase

(3) Transportation of Oxygen
ex. hemocyanin

(4) Preservation of Copper
ex. Cu-thioneine

Classification of Copper Proteins

	EPR	Color	Oxidation state	Number
Type-1	+	blue	Cu(II)	mononuclear
Type-2	+	non blue	Cu(II)	mononuclear
Type-3	-	non blue	Cu(II)-Cu(II)	binuclear

The coefficient of visible absorption spectra of a typical blue copper protein is generally from 50 to 100 times as strong as that of generals Cu(II) complex with $\varepsilon(600)$ of 1000-5000. Fig. 1-2 (a) shows the visible absorption spectra of one of blue copper protein, pseudoazurin from *methylobacterum extorquens* AM1 (PAZAM1).

Fig. 1-2 (b) shows the EPR spectrum of PAZAM1 and the characteristic small hyperfine splitting in $A_{||}$ is clearly confirmed. Because the copper atom in oxidized state has nine d electrons, its $d_{x^2-y^2}$ orbital is unoccupied. This is why the EPR spectrum originates from the spin of the unpaired electron coupling to the nuclear spin of the copper atom, but the small hyperfine splitting is not able to be explained clearly. This narrow hyperfine splitting is not found in other normal copper proteins.

The high redox poteintial of blue copper proteins is also characteristic property. The intense absorption band, irregularly narrow hyperfine splitting and high redox potential are necessary to characterize the blue copper proteins.

1-3 History of the Structural Studies on Blue Copper Proteins

The first crystal structure of blue copper protein is of plastocyanin that was revealed at 2.7Å in 1984 (Freeman, 1978). The refined structure of palstocyanin at 1.33Å was reported in 1992 (Guss & Freeman, 1992). Until now two azurin structures, one pseudoazurin structure and one amicyanin were analyzed at atomic level by X-ray crystallography. In this work these crystal structures

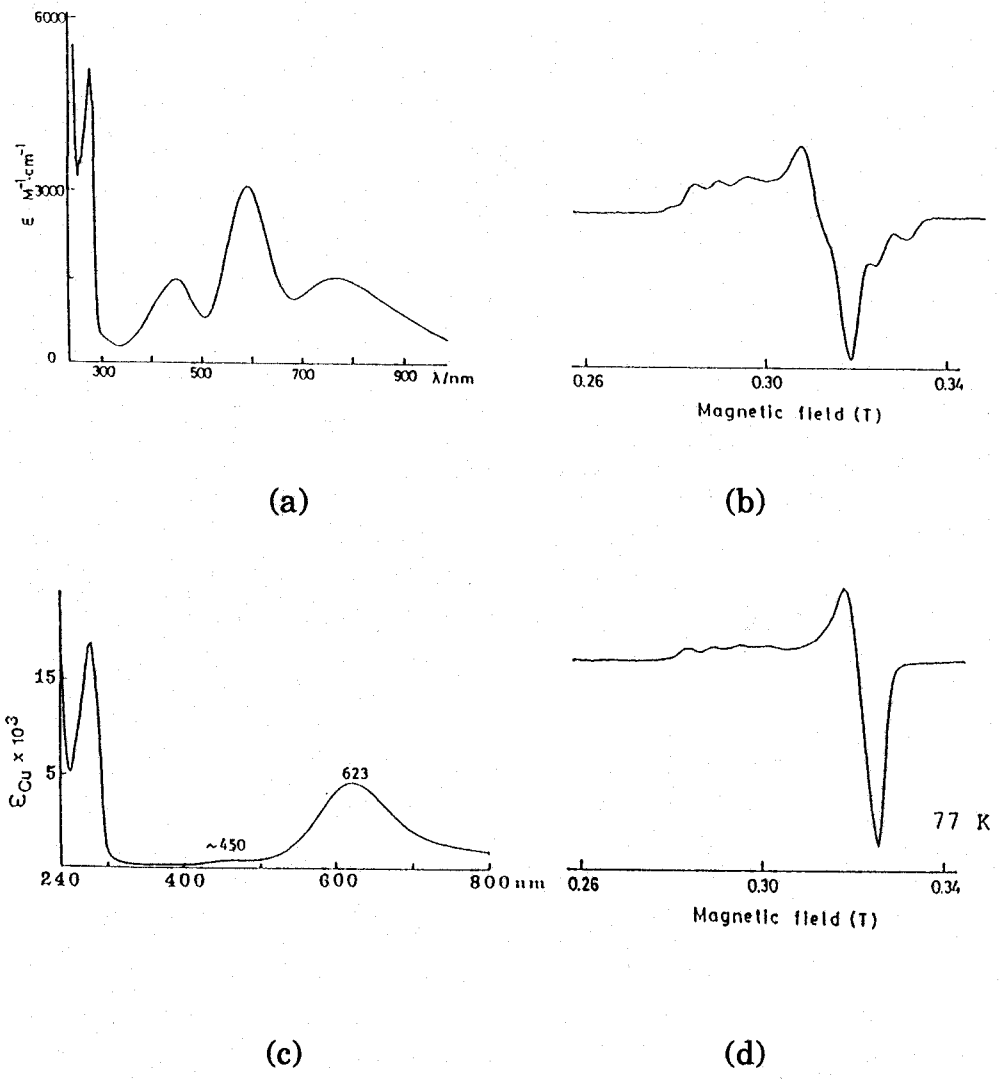

Fig. 1-2 Comparison of visible absorption spectrum and EPR spectrum between pseudoazurin from *methylobacterium extorquens* AM1 (a & b) and azurin from *achromobacter xylosoxidans* NCIB11015 (c & d)

were used as the starting models in order to solve the crystal structures which were crystallized in this work.

The amino acid sequence of pseudoazurins from three different sources, *Methylobacterium extorquens* AM1 (PAZAM1, Ambler & Tobari, 1985), *Alcaligenes faecalis* S-6 (PAZS6; Homel, Adman, Walsh, Beppu & Titani, 1986) and *Achromobacter cycloclastes* IAM1013 (PAZIAM, Ambler, 1977), has been reported. Among these proteins, PAZS6 is the only one the crystal structure of which has been determined by X-ray diffraction method at 2.0Å resolution (Adman *et al.*, 1989). In this work, the molecular structure of PAZS6 was used as the initial model for the molecular replacement method to solve the crystal structure of PAZAM1 and PAZIAM.

The sequence of azurins from 9 different sources has been reported in NBRF data bank in 1993 and of which two azurin structures were analyzed. One is from *alcaligenes denitrificans* NCTC8582 at 1.8Å resolution (AZUNCTC; Baker, E. N. 1988) and the other is from *pseudomonas aeruginosa* at 3.0Å resolution (AZUAERU; Adman, E. T., 1978). In this work the crystallized azurin is from *achromobacter xylosoxidans* NCIB11015, which was previously called Iwasaki's *pseudomonas denitrificans* or *alcaligenes sp.* and the structure of *alcaligenes denitrificans* NCTC8582 was used as the starting model in molecular replacement method.

2 Preliminary X-ray Studies and Data Collection

2-1 Crystallization of Blue Copper Proteins

2-1-1 Crystallization of PAZAM1

Methylobacterium extorquens AM1 is one of the methylotrophic bacteria, which grows on C_1 compound like methylamine, formaldehyde, methanol as the sole carbon and energy source. When the bacterium is cultivated in the medium containing methylamine together with copper ion at normal concentration (< 0.1mg/l), methylamine dehydrogenase (MADH) and a blue copper protein named amicyanin are produced. On the other hand, when the culture medium contains copper at high concentration (> 1mg/l), little amount of amicyanin and large amount of another blue copper protein named pseudoazurin are synthesized (Tobari, 1984). Pseudoazurin is quite different from amicyanin concerning molecular weights, amino acid sequences, absorption and EPR spectrum. Recently, MADH and amicyanin were co-crystallized (Chen, Louis, Mathews, Davidson & Husain, 1988) and its X-ray structure revealed amicyanin as the first electron acceptor from MADH (Chen *et. al.*, 1993). Pseudoazurin is reported to take another location in the electron transport chain of *Methylobacterium extorquens* AM1

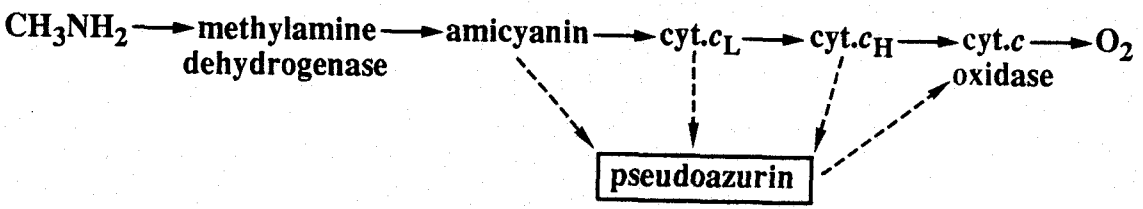

⟶ low Cu concentration in the medium
⇢ high Cu concentration in the medium
cyt.c_H ; pI ~ 9
cyt.c_L ; pI ~ 4

J.Tobari, "Microbial Growth on C_1 Compounds"
(eds., R.L.Crawford and R.S.Hason) 1984

Fig. 2-1 Proposed electron transportation chain in methylotrophic bacterium, *methylobacterium extorquens* AM1 growing on methylamine.

growing on methylamine and excess amount of copper (Tobari, 1984)(Fig. 2-1).

PAZAM1 was purified and characterized as described previously (Ambler & Tobari, 1985). Single crystals were obtained by the hanging-drop vapor diffusion technique with ammonium sulfate as a precipitant reagent at 20 °C. A 6 μl droplet of 15 mg/ml protein solution containing 50 mM potassium phosphate (pH 8.0), 1 mM sodium azide and 40% saturated ammonium sulfate was set as the hanging drop against 500 μl reservoir solution containing 50 mM potassium phosphate (pH 8.0), 1 mM sodium azide and 67% saturated ammonium sulfate. After a few days, small number of crystals with maximum dimensions of 0.5 × 0.5 × 1.5 mm appeared in the droplet (Fig. 2-2).

2-1-2 Crystallization of PAZIAM

Achromobacter cycloclastes IAM 1013 is one of denitrifying bacteria. The crystallographic studies of the nitrite reductase (NIR) and the blue copper protein named pseudoazurin from this bacteria have been carried out by Turley & Adman (Turley, S. & Adman, E. T., 1988). However, the crystal of pseudoazurin reported was so thin that the data collection has not been proceeded.

The cultivation of *Achromobacter cycloclastes* IAM1013, and the

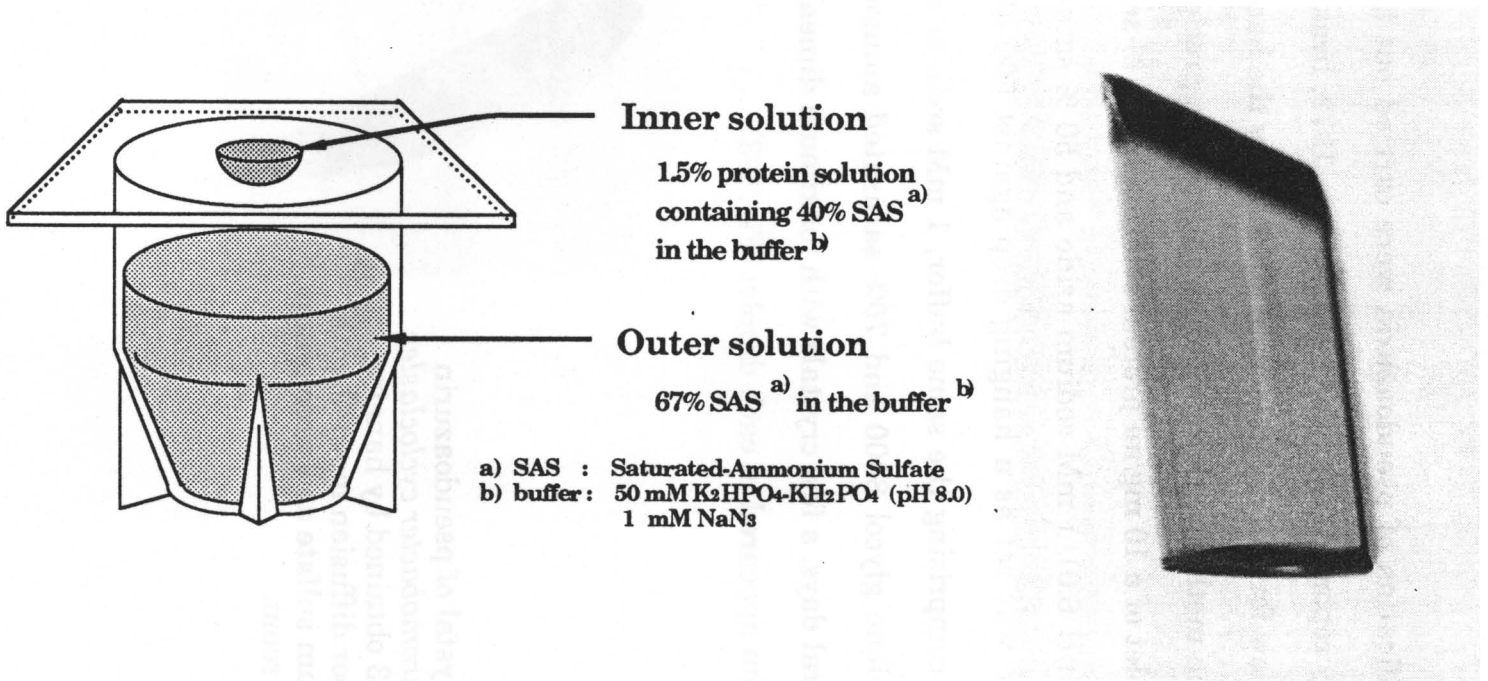

Fig. 2-2 Crystallization of pseudoazurin from *methylobacterium extorquens* AM1. When the hanging-drop vapor diffusion method was applied, a few crystals with maximum dimensions of 0.5 × 0.5 × 1.5 mm grew in the inner solution within 1 day.

isolation and purification of pseudoazurin were carried out by the methods previously reported (Iwasaki & Matsubara, 1972, Iwasaki & Shidara 1975). A new form of crystals were obtained by the hanging-drop vapor diffusion method with ammonium sulfate as a precipitant at 4°C. A 6 μl droplet of a 10 mg/ml protein solution in 0.1 M sodium cacodylate buffer (pH 6.0), 1 mM sodium azide and 50 % saturated ammonium sulfate was set as a hanging drop against 500 μl of a reservoir solution comprising the same buffer, 1 mM sodium azide, 5% (w/v) polyethylene glycol 8000 and 70% saturated ammonium sulfate. After several days, a few crystals with maximum dimensions of $0.3 \times 0.4 \times 0.9$ mm appeared in each droplet (Fig. 2-3).

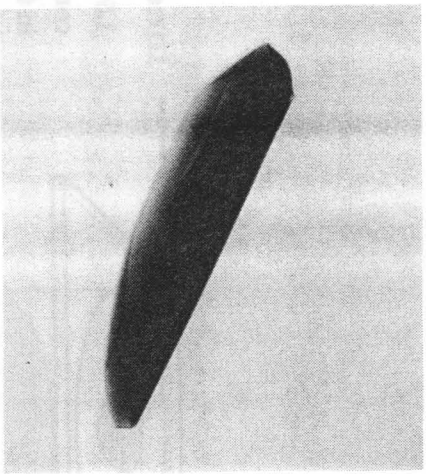

Fig. 2-3 A crystal of pseudoazurin from *achromobacter cycloclastes* IAM 1013 obtained by hanging drop-vapor diffusion method with ammonium sulfate as a precipitant in a cold room.

2-1-3 Crystallization of AZUNCIB

Achromobacter xylosoxidans NCIB11015 is one of the denitrifying bacteria and the crystallographic studies of the blue copper protein named azurin from this bacteria has been carried out by Strahs (Strahs, G., 1969) and Baker (Norris & Baker, 1979). The crystals of azurin reported, although, were so thin that the data collection has not been proceeded.

Many kinds of precipitants in the conventional method, although, small crystals always grew to long needles or thin plates. To give rise to sufficiently large single crystals, seeding method is tried (Thaller, C. *et al.*, 1985).

Fig. 2-4 shows the crystallization of AZUNCIB by macro-seeding method with ammonium sulfate as a precipitant to obtain some suitable crystals. Small crystals which had been grown by the first crystallization using hanging-drop vapor diffusion method were washed several times in the washing solution. A washed seed was injected into a solution containing protein and precipitant. Several times of the application for the macro-seeding technique many suitable crystals were obtained.

Fig. 2-5 shows the crystal growth of AZUNCIB. One half of the last crystal was used to take two precession photographs and the other was used to collect the X-ray diffraction data.

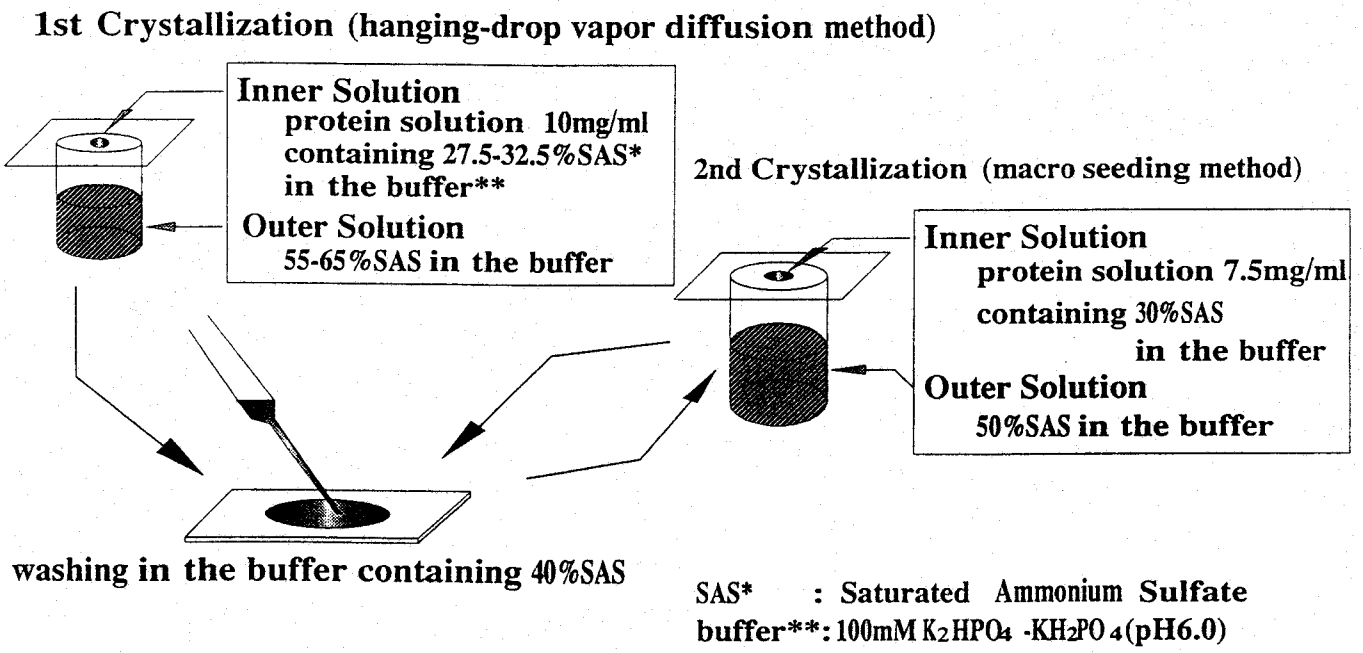

Fig. 2-4 Condition of Macro Seeding Method for Crystallization of Azurin from Achromobacter xylosoxidans NCIB11015. Washing process is most important to obtain some suitable crystals of azurin. After several times of seeding, azurin crystals grew more than $0.25 \times 0.25 \times 1.5$ mm (Fig. 2-5).

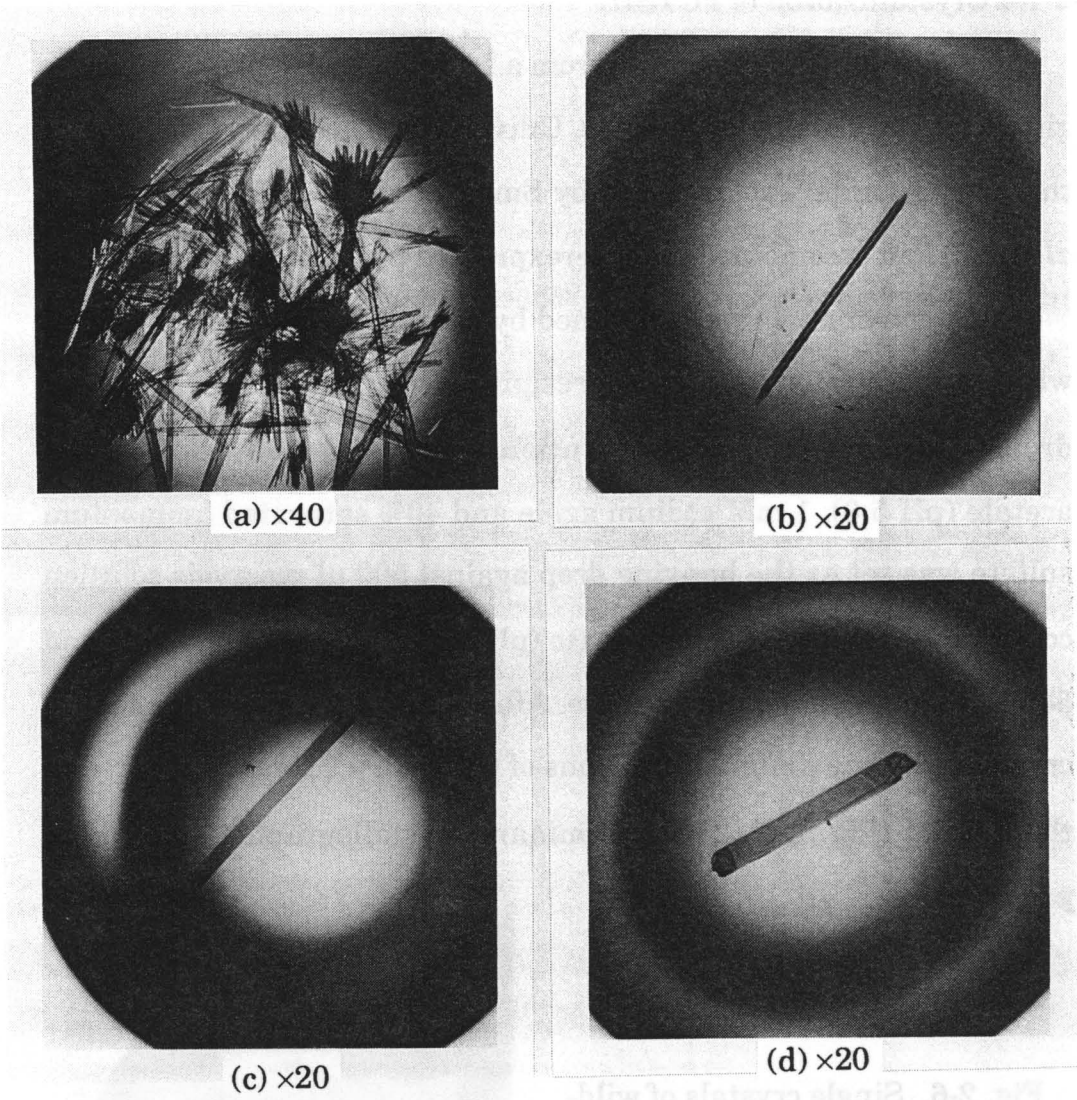

Fig. 2-5 Crystallization of azurin from *achromobacter xylosoxidans* NCIB 11015. The crystals were grown by the macro-seeding method step by step. The final crystal used in data collection had a dimension of 0.25 x 0.25 x 1.5 mm.

2-1-4 Crystallization of PCYSIL

A wild-type plastocyanin from a high plant of *silene* was kindly gifted by Dr. Takabe of Meijyou University. The precursor gene of this plastocyanin was analyzed by Smeekens *et al.* (Smeekens, S. *et al.* 1985) and recombined and overexpressed by Takabe.

Single crystals were obtained by the vapor diffusion technique with ammonium sulfate as a precipitant reagent at 20 °C. A 6 μl droplet of 5 mg/ml protein solution containing 100 mM sodium acetate (pH 5.0), 1 mM sodium azide and 40% saturated ammonium sulfate was set as the hanging drop against 500 μl reservoir solution containing 100 mM sodium acetate (pH 5.0), 1 mM sodium azide and 54% saturated ammonium sulfate. After a few days, small number of crystals with maximum dimensions of 0.4 × 0.4 × 0.6 mm appeared in the droplet (Fig. 2-6). The preliminary crystallographic study is in progress.

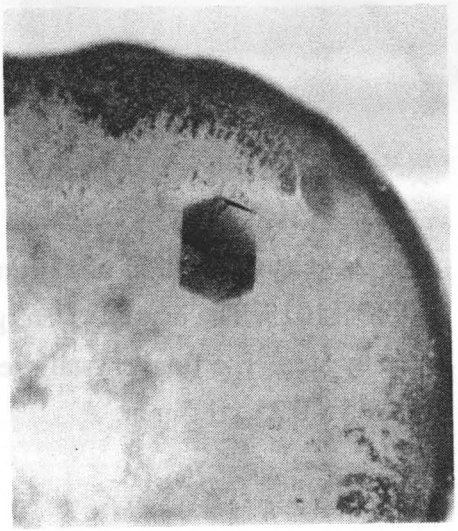

Fig. 2-6. Single crystals of wild-type plastocyanin from silene were obtained by hanging-drop vapor diffusion method with ammonium sulfate as a precipitant reagent at pH 5.0.

2-2 Preliminary X-ray Studies on Three Blue Copper Proteins

Preliminary crystallographic data of three blue copper proteins except PCYSIL were determined using a precession camera with CuKa radiation from a rotating anode X-ray generator (fine-focused beam, β–filtered, 40 kV, 100 mA, Rigaku RU-300).

The crystals of PAZAM1 belong to the orthorhombic system of space group $P2_12_12_1$ determined by using the precession photoes (Fig. 2-7). The unit cell dimensions are obtained as a= 52.619(4), b= 63.280(6) and c= 35.133(2)Å (1Å = 0.1 nm) determined by least-squares refinement of the 2θ values of 40 reflections. The size of the unit cell indicates one pseudoazurin molecule in the asymmetric unit and 1.8$Å^3$ per dalton of protein. Solvent thus occupies approximately 44% of the unit cell volume (Matthews, 1968).

From the Laue symmetry and the systematic absences of reflections, the PAZIAM crystal was found to have the orthorhombic crystal lattice with space group $P2_12_12_1$ (Fig. 2-8). The unit cell parameters were determined to be a= 56.69(2) Å, b= 61.53(2) Å, and c= 30.20(1) Å (1 Å = 0.1 nm) by least-squares refinement of the 2θ values of 25 reflections measured with a diffractometer. When the asymmetric unit of the crystal lattice includes one pseudoazurin molecule (molecular mass = 12,900 dalton), the crystal volume per

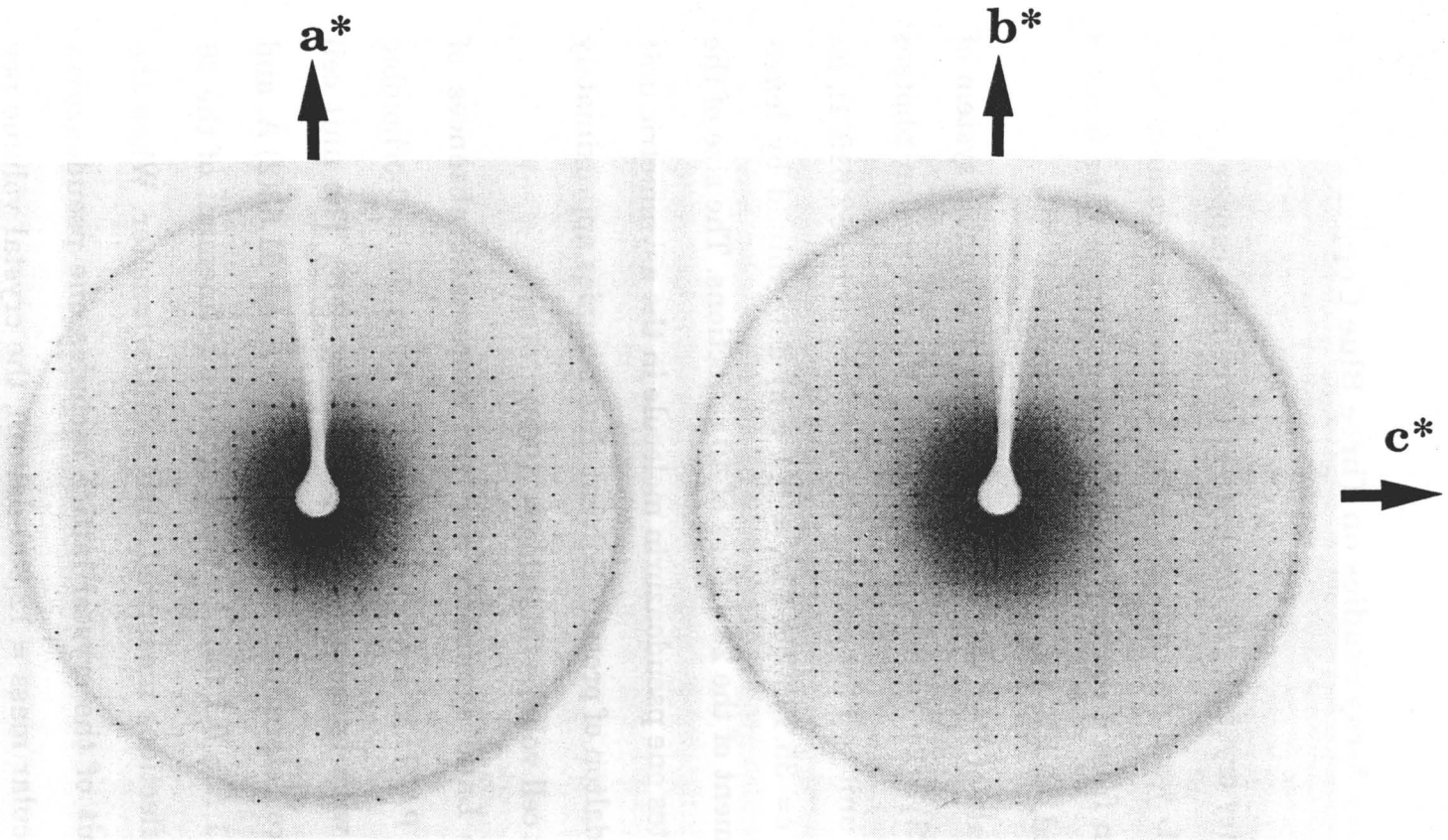

Fig. 2-7 Precession photographs of pseudoazurin from *methylobacterium extorquens* AM1 (PAZAM1)

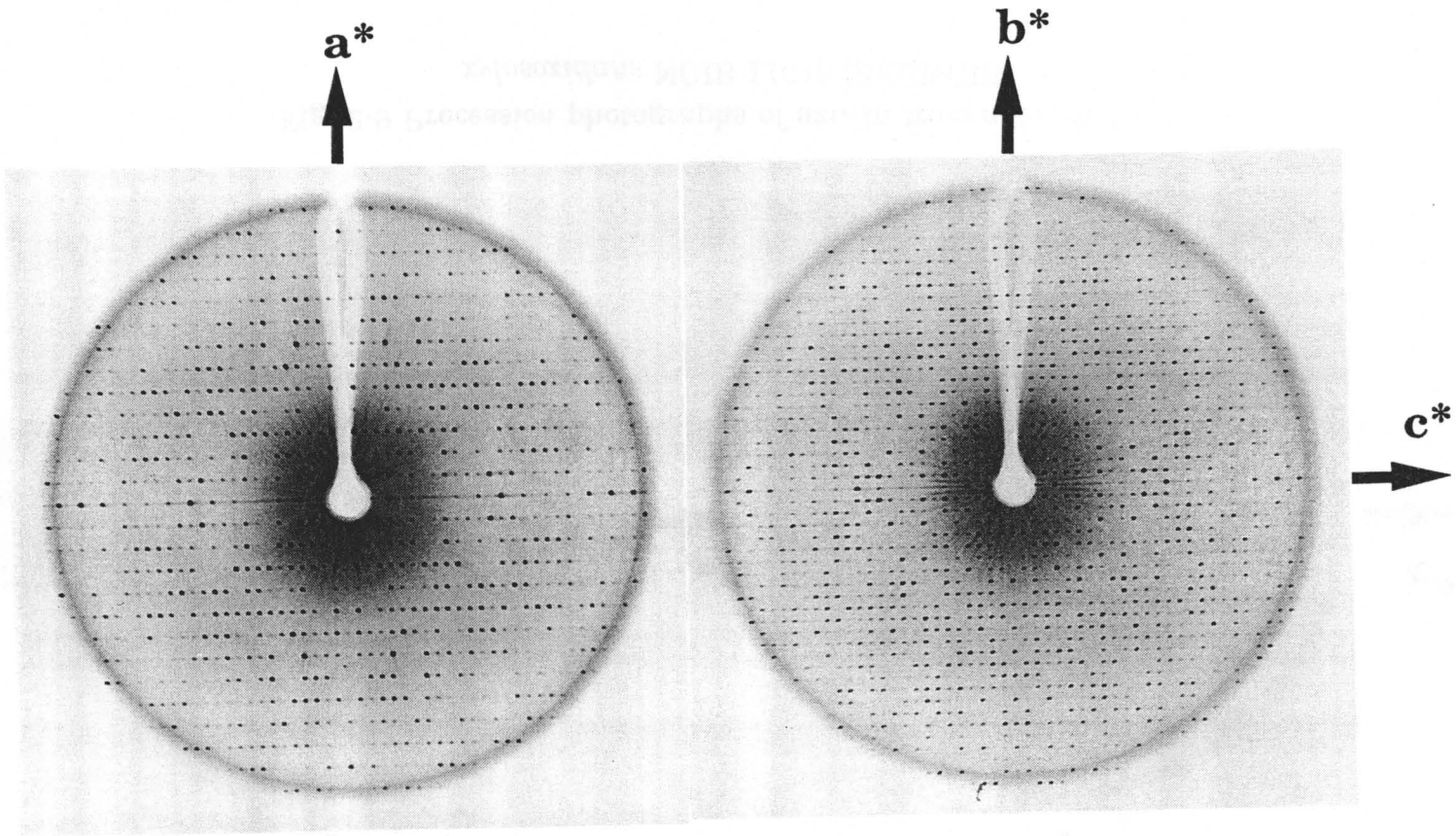

Fig. 2-8 Precession photographs of pseudoazurin from *achromobacter cycloclastes* IAM 1013 (PAZIAM)

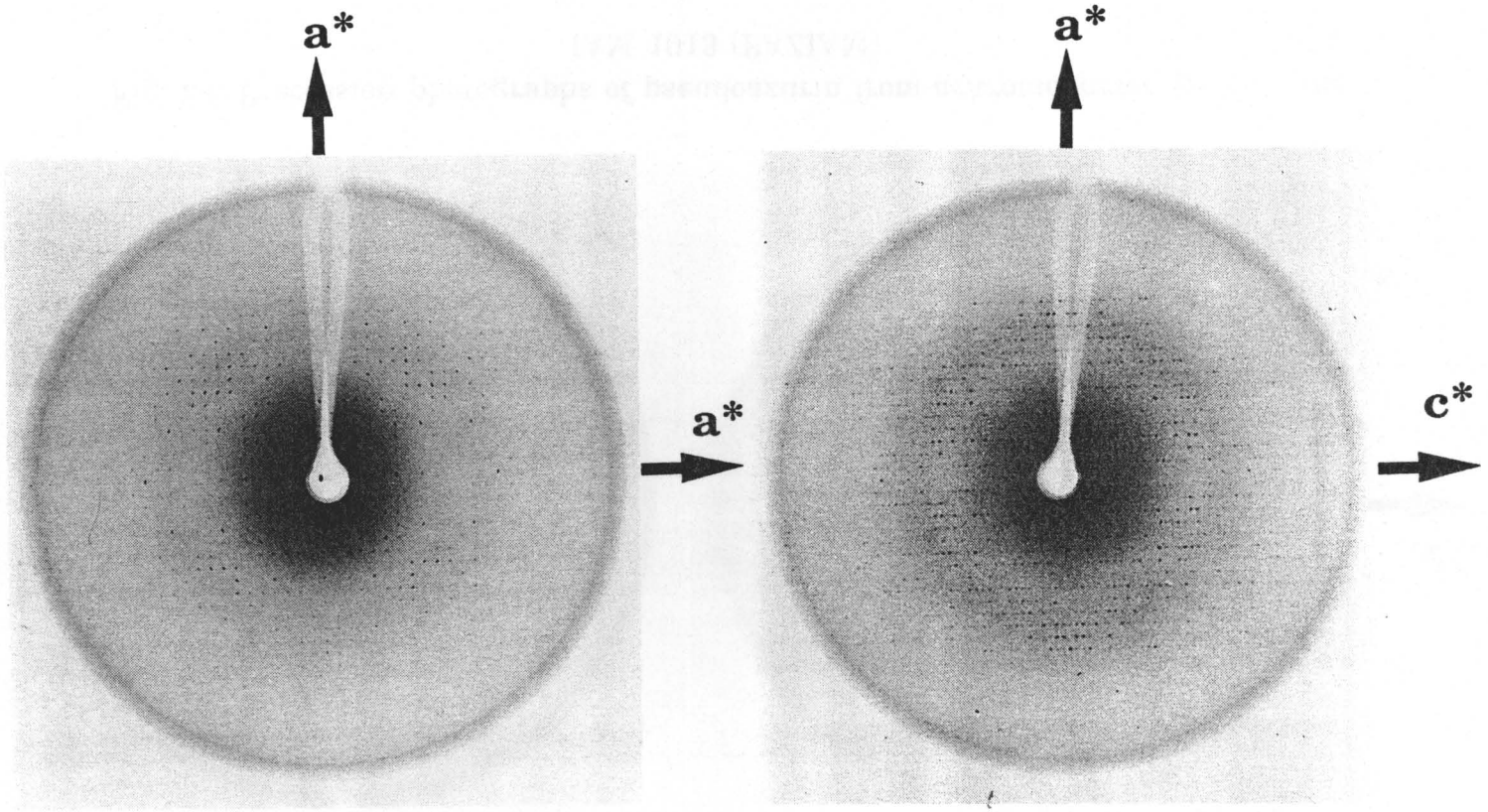

Fig. 2-9 Precession photographs of azurin from *achromobacter xylosoxidans* NCIB 11015 (AZUNCIB)

unit molecular mass (Vm) has the reasonable value of 2.04 $Å^3$/dalton (Matthews, 1968).

From the Laue symmetry and the systematic absences of reflections, the AZUNCIB crystal was found to have the tetragonal crystal lattice with space group $P4_122$ (or $P4_322$) (Fig. 2-9). The unit cell parameters were determined to be a= 52.3Å, b= 52.3(2) Å, and c= 100.2(1) Å (1 Å = 0.1 nm) by the precession photos. When the asymmetric unit of the crystal lattice includes one pseudoazurin molecule (molecular mass = 14,000 dalton), the crystal volume per unit molecular mass (Vm) has the reasonable value of 2.4 $Å^3$/dalton (Mattews, 1968).

Summary of the crystallographic data of three blue copper proteins are listed in Table. 2-1.

Table 2-1 *Crystallographic Data of Three Blue Copper Proteins*

	PAZAM1	PAZIAM	AZUNCIB
Crystal system	orthorhombic	orthorhombic	tetragonal
Space group	$P2_12_12_1$	$P2_12_12_1$	$P4_122(P4_322)$
Cell constants (Å)			
a =	52.619(4)	56.69(2)	52.3
b =	62.280(3)	61.53(2)	52.3
c =	35.133(3)	30.20(1)	100.2
No. of molecules (/ asym. unit)	1	1	1
Value of Vm (Å*3/dalton)	2.18	2.04	2.4
Solvent content (%)	44	40	50

2-3 Data Collection of Three Blue Copper Proteins

2-3-1 PAZAM1

In order to proceed the multiwavelength dispersion study, two intensity data at two wavelegths monochromatized by a Si(111) monochromator system were collected with synchrotron radiation at the BL6A2 station of 2.5 GeV energy produced by the storage ring in the Photon Factory, the National Laboratory for High Energy Physics (KEK), Tsukuba, Japan (Table 2-2). The first one (Native-I) is taken at λ_1=1.04Å, and the second (Native-II) at λ_2=1.375Å, which is just below the *K* absorption edge of copper atom (λ_e=1.388Å).

Diffraction patterns were recorded on the Fuji Imaging-Plate (IP, 200 × 400mm, Fuji Photo Film) (Miyahara *et al.*, 1986) using the Sakabe's Weissenberg camera for macromolecules (Sakabe, 1991; Sakabe, 1983) with an aperture collimator of 0.1 mm diameter and a cylindrical cassette of 286.5 mm radius filled with helium gas. The read-out of IP data were carried out by a system of Fujix BA100 (Fuji Photo Film) and the intensity data were processed using the *WEIS* program system (Higashi, 1989). R_{merge} for the data collected at λ_1 and λ_2 were 8.7% for 25154 reflections up to 1.2Å resolution data, and 8.7% for 19846 reflections up to 1.2Å resolution data, respectively (Table. 2-3).

Another three sets of intensity data from a native crystal (Native-III) and two heavy atom derivatives of PAZAM1 (Deriv-U and Deriv-Pt) were measured on a single crystal diffractometer (Table 2-4). A platinum derivative was obtained by soaking native crystals in a solution containing 5mM K_2PtCl_4 for one day, while a uranium derivative was obtained at first by transferring the native crystal to ammonium acetate buffer solution containing 70% saturated ammonium sulfate and then to a solution containing 10mM $UO_2(AcO)_2$ for one day. The data collections of these crystals were performed on a Rigaku four-circle diffractometer with β–filtered CuK_α radiation from rotating anode X-ray generator (40kV, 200mA).

Table 2-2. *Experimental conditions of data collection for native crystals of PAZAM1 using synchrotron radiation*

X-ray source	Synchrotron radiation (at Photon Factory, KEK, Japan)			
Camera	Sakabe's Weissenberg camera			
Detector	Imaging Plate (IP; 200 × 400 mm) & BA100 system			
Crystal to film distance (mm)	286.5			
Collimator	0.1 mm diameter			
Data Set	Native-I		Native-II	
Wavelength (Å)	λ =1.04		λ =1.375	
Coupling const. (deg/mm)	2.0	2.0	2.0	2.0
Number of crystal used	1	1	1	1
Rotation axis	*b*	*c*	*a*	*c*
Oscillation angle (deg/sheet)	11.0	13.5	14.0	10.5
Total oscillation angle (deg)	209	216	196	199.5
Total exposure time (sec)	522.5	540	490	498.75

Table 2-3. *Results of data reduction for native crystals of PAZAM1*

Data Set			Native-I (at λ_1=1.04Å)		Native-II (at λ_2=1.375Å)	
Resolution range(Å)			No. of reflections observed	*R*sym (%)	No. of reflections observed	*R*sym (%)
	-	15.0	131	7.0	115	9.5
15.0	-	7.5	1020	6.7	702	7.1
7.5	-	5.0	3082	7.4	2351	6.4
5.0	-	3.8	4096	5.8	3800	5.4
3.8	-	3.0	6975	6.6	6015	5.8
3.0	-	1.2	50881	3.9	38489	11.9
No. of total measured reflections				94051		62302
No. of total independent reflections				25154		19846
No. of total reflections with A. D.				11778		9320
R_{merge}(%)				8.7		8.7

Table 2-4. *Results of data collection for native crystal and heavy atom derivatives using Rigaku four-circle diffractomater(PAZAM1)*

Data Set	Native-III	Deriv-U	Deriv-Pt
No. of crystal used	1	1	1
No. of observed reflections*	14375	7050	9822
No. of independent reflections	13902	6474	8793
Maximum 2θ value (deg)	54.2	33.7	38.2
Resolution (Å)	1.68	2.70	2.35
Total Radiation damage (% in $\|F\|$)	5.4	10.0	8.0

* Intensity data were measured by ω-scan method using CuK_α radiation (40kV, 200mA, β-filter)

2-3-2 Data Collection for PAZIAM

X-ray intensity measurements for PAZIAM have been carried out up to 2.0Å resolution with a four-circle diffractometer (Rigaku AFC-5R) using Ni-filtered Cu$K\alpha$ radiation (normal focused beam, 40 kV, 300 mA., Rigaku RU-300). A total of 4,710 unique reflections was collected within 10% decay of an average structure amplitude of monitor reflections compared with its starting value.

Another set of diffraction data for PAZIAM up to 1.54Å resolution was obtained using an imaging plate detector operated in the Rigaku RAXIS-IIc system with graphite monochromated Cu$K\alpha$ radiation from a 12 kW rotating anode generator. The crystal to detector distance was set at 71.5 mm. Diffraction data were collected for a single crystal rotated about its *b* axis. The total exposures were recorded on 38 plates covering the total rotation range of 90°. Among 28,799 accepted observations up to 1.54Å resolution, 10,643 independent reflections were obtained, the completeness of which was 64.7% with a R_{merge} of 4.2%. To improve the completeness, the two data sets were merged and scaled together using the program, *PROTEIN* (Steigemann, 1974). The completeness for all data up to 1.54Å became 84.5% with a R_{merge} of 3.0%.(Table 2-5, 2-6, 2-7)

Table 2-5. *Experimental Conditions of Data Collection for PAZIAM*

Device	RAXIS-IIc (RIGAKU)
X-ray	CuKa (1.54178Å 40kV, 100mA)
Detector	IP (Fuji, imaging-plate)
Crystal-film distance (mm)	71.5
Number of crystal used	1
Rotation axis	*b*
Exposure time (min/sheet)	15.5
Total oscillation angle (deg)	90

Table 2-6. *Results of data collection for PAZIAM using RAXIS-IIc system*

Resolution range (Å)			No. of reflections observed	No. of reflections theoretical	completeness (%)	R_{merge} (%)
	-	5.00	22	562	3.9	3.2
5.00	-	3.00	109	1806	6.0	1.3
3.00	-	2.50	1047	1627	64.4	3.2
2.50	-	2.20	1692	1788	94.6	3.6
2.20	-	2.00	1720	1849	93.0	4.2
2.00	-	1.90	1094	1197	91.4	5.0
1.90	-	1.80	1373	1532	89.6	6.6
1.80	-	1.70	1628	1723	87.1	8.5
1.70	-	1.60	1393	2364	58.9	10.8
1.60	-	1.54	540	1723	31.3	12.6
1.54	-	1.538	25	129	19.4	17.3

No. of total measured reflections	28799
No. of total independent reflections	10643
Completeness (%)	64.7
R_{merge}(%)	4.2

Table 2-7 *Results ofdata collection for PAZIAM using Rigaku four-circl diffractometer*

Four-circle diffractometer (RIGAKU, AFC-5R) 2θ-omega scan, CuK α(λ= 1.54178Å), 40kV, 300mA, Ni-filter	
No. of crystal used	1
No. of observed reflections	4820
No. of independent reflections	2405
Maximum 2θ value (deg)	30.0
Resolution (Å)	2.0
Total Radiation damage (% in |F|)	9.7

2-3-3 Data Collection for AZUNCIB

The intensity data set of AZUNCIB was collected at λ_1=1.00Å with synchrotron radiation at the Photon Factory using the Sakabe's Weissenberg camera for macromolecules (Sakabe, 1991; Sakabe, 1983) with a cylindrical cassette of 430.0 mm radius. Diffraction data were collected for a single crystal rotated about its a and *c* axis. The total exposures were recorded on 11 and 15 plates covering the total rotation range of 180° and 90°, respectively (Table 2-8). Among 101,192 accepted observations up to 2.5Å resolution, 9,964 independent reflections were obtained with the R_{merge} for the data was 8.9 %(Table 2-9).

Table 2-8 *Conditions of Data Collection for AZUNCIB*

X-ray	Synchrotron radiation	
Wave length (Å)	1.00	
Camera	Weissenberg camera for pmacromolecules	
Crystal-film distance (mm)	430	
Rotation axis	a	c
Crystal oscillation angle (deg.)	17.0	8.92
Weissenberg coupling constant (deg./mm)	2.0	2.0
No. of crystal used	1	1
Total oscillation angle (deg.)	182.0	126.8
Total exposure time (sec)	935	669

Table 2-9 *Statistics of Data Collection for AZUNCIB*

Resolution range (Å)	No. of reflecions observed	Rsym (%)
- 15.0	481	7.1
15.0 - 7.5	3572	6.4
7.5 - 5.0	10072	7.2
5.0 - 3.8	16846	6.9
3.8 - 3.0	22126	9.1
3.0 - 2.5	47480	17.1

3 Structure Analysis and Refinement

3-1 Molecular Replacement Method

Three crystal structures have been solved by the molecular replacement method using the program of *MERLOT* program package (Fitzgerald, 1988). The rotation and translation parameters were calculated using *CROSUM* (Crowther, 1972) and *RVAMAP* function, respectively, and those parameters thus obtained were refined by *RMINIM*. (Ward *et al.*, 1975) function.

For both PAZAM1 and PAZIAM, the molecular structure of PAZS6 was used as the starting model, and for the calculation of AZUNCIB, the molecular structure of azurin from *Alcaligenes denitrificans* NCTC8582 (Baker, 1987, AZUNCTC) was used as the starting model, respectively.

The ratios of identical *vs.* total residues are 55/123 (45%) between PAZS6 and PAZAM1, 81/123 (66%) between PAZIAM and PAZS6, 90/129 (70%) between AZUNCIB and AZUNCTC, respectively (Fig. 3-1 & 3-2).

3-1-1 Molecular Replacement Method for Analyzing of PAZAM1

The site of the copper atom in the native crystal of PAZAM1

```
                1         10        20        30        40        50        60
PAZS6      ENIEVHMLNK GAEGAMVFEP AYIKANPGDT VTFIPVDKGH NVESIKDMIP EGAEKFKSKI
PAZAM1     DEVAVKMLNS GPGGMMVFDP ALVRLKPGDS IKFLPTDKGH NVETIKGMAP DGADYVKTTV
PAZIAM     ADFEVHMLNK GKDGAMVFEP ASLKVAPGDT VTFIPTDKGH NVETIKGMIP DGAEAFKSKI

               61        70        80        90       100       110       120
           NENYVLTVTQ PGAYLVKCTP HYAMGMIALI AVGDSPANLD QIVSAKKPKI VQERLEKVIA SAK
           GQEAVVKFDK EGVYGFKCAP HYMMGMVALV VVGDKRDNLE AAKSVQHNKL TQKRLDPLFA QIQ
           NENYKVTFTA PGVYGVKCTP HYGMGMVGVV EVGDAPANLE AVKGAKNPKK AQERLDAALA ALGN
```

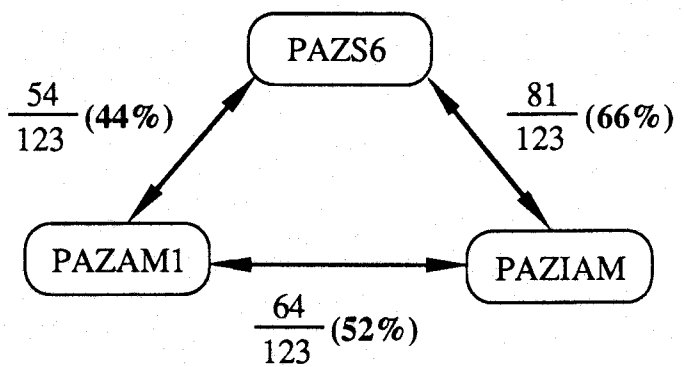

PAZS6 *Alcaligenes faecalis* S-6

PAZAM1 *Methylobacterium extorquens* AM1

PAZIAM *Achromobacter cycloclastes* IAM1013

Fig. 3-1 Amino acid sequences of three pseudoazurins . The thick characters are the conserved amino acids and % mean the total homology among pseudoazurins.

1. *Pseudomonas aeruginosa* P6009
2. *Pseudomonas denitrificans* NCIB9496
3. *Pseudomonas fluorescens* B-93
4. *Pseudomonas fluorescens* C-18
5. *Pseudomonas fluorescens* D-35
6. *Bordetella bronchiseptica* NCTC8344
7. *Alcaligenes denitrificans* NCTC8582
8. *Alcaligenes faecalis* NCIB8156
9. *Achromobacter xylosoxidans* NCIB11015

Sequences Homology between No. 7 and No. 9

```
      1       10        20        30        40        50        60
No. 7 AQCEATIESN DAMQYNLKEM VVDKSCKQFT VHLKHVGKMA KAVMGHNWVL TKEADKEGVA
      * *   * * * **   **   * *******  * *** ** *  * ********  ** **  *
No. 9 AECSVDIAGN DQMQFDKKEI TVSKSCKQFT VNLKHPGKLA KNVMGHNWVL TKQADMQGAV

     61       70        80        90       100       110       120
      TDGMNAGLAQ DYVKAGDTRV IAHTKVIGGG ESDSVTFDVS KLTPGEAYAY FCSFPGHWAM
       *** ***   ***  * **  ********** * ********  **  ** ***  ******* *
      NDGMAAGLDN NYVKKDDARV IAHTKVIGGG ETDSVTFDVS KLAAGEDYAY FCSFPGHFAL

    121
      MKGTLKLSN
      *** ***
      MKGVLKLVD
```

90/129 (70%)

No. 7 *Alcaligenes denitrificans* NCTC8582 *cf.* Baker,E.N. 1.8Å resolution (1988)
No. 9 *Achromobacter xylosoxidans* NCIB11015

Fig. 3-2 Amino acid sequences of nine azurins are known in SWISS sequence data bank in 1993. Sequence homology between AZUNCIB (No. 7) and AZUNCTC (No. 9) is shown.

was obtained from the difference Patterson maps calculated with the synchrotron radiation data containing multiwavelength anomalous dispersion effect. When the copper site of the starting model is set to the origin of the unit cell, the distance from the origin to the copper site in the native crystal of PAZAM1 is just equal to the translation parameter for the molecular replacement method. Only the rotation search could solve the structure of PAZAM1. The crystal structure analysis of PAZAM1 was carried out by the following steps.

I. The position of copper atom in the native crystal was determined from the difference Patterson maps with anomalous dispersion data (Native-I; λ=1.04Å and Native-II; λ=1.375Å).

II. The position of copper atom was confirmed in the electron density maps phased by two heavy atom derivatives (Native-III, Deriv-U and Deriv-Pt).

III. Based on the position of copper atom, molecular replacement method was carried out . The initial translation parameters were set to the same distance between two copper sites in the native crystal and in the model structure. The rotation and translation parameters thus obtained were refined by *RMINIM* (Ward *et al.*, 1975) function.

I.. Determination of copper site

The difference Patterson maps in the Harker sections with coefficients of (a) $[F(\lambda_1)^+ - F(\lambda_1)^-]^2$, (b) $[F(\lambda_1)^+ - F(\lambda_2)^-]^2$ and (c) $[F(\lambda_2)^+ - F(\lambda_2)^-]^2$ were calculated with the synchrotron data up to 6.0Å resolution, where F^+ and F^- stand for the structure amplitude of Bijvoet related reflections, and λ_1 and λ_2 correspond to the X-ray wavelength of 1.04Å and 1.375Å, respectively. Fig. 3-3 shows three Patterson maps in the Harker section of V=1/2 with the respective coefficients. Among small number of noisy peaks the highest single peak appeared in the Fig. 3-3(a), which was corresponding to the highest peaks in other Harker sections and they were assigned to the copper cross vectors. The position of copper atom thus determined was x=0.27, y=0.26 and z=0.60 in fractional coordinates of the unit cell. The position was also confirmed in the Patterson maps of Fig. 3-3(b) and 3-3(c), although, the corresponding peaks are not as high as the peaks in Fig. 3-3(a).

After the refinement of Cu^{2+} positional parameters, phases were calculated by MAD method using the copper atom as a heavy-atom against the 10,205 reflections between 10.0-4.0Å resolution. The occupancy of 0.80 (23.3/29) with B-factor of 19.6Å^2 and the figure of merit of 0.41 were obtained. Even though the calculated electron density on mini maps revealed the β–barrel structure the

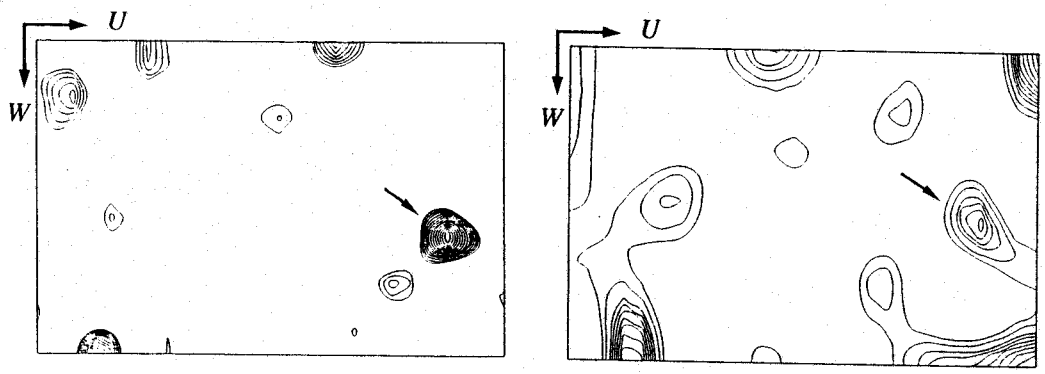

(a) (b)

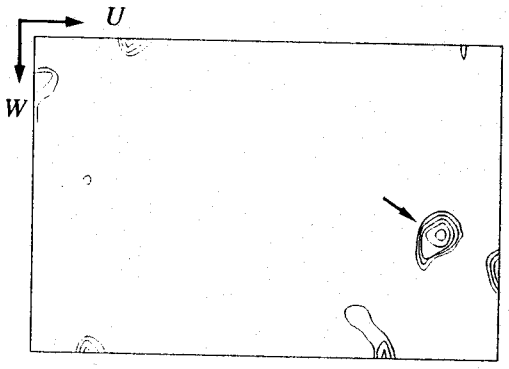

(c)

Fig. 3-3 Patterson maps in the Harker section of V=1/2 with coefficients of (a) $[F(\lambda_1)^+ - F(\lambda_1)^-]^2$, (b) $[F(\lambda_1)^+ - F(\lambda_2)^-]^2$ and (c) $[F(\lambda_2)^+ - F(\lambda_2)^-]^2$, where λ1 and λ2 stand for 1.375Å and 1.04Å, respectively. The positions of copper atom self-vectors are marked by arrow.

confirmation of the residues was so difficult that the model-building was not processed.

II. Confirmation of copper site by the MIR method

After scaling the diffractometer data from the native and two heavy atom derivatives, the mean differences in the isomorphous structure factors were calculated as 27% for the uranium derivative and 13% for the platinum derivative, respectively (Table 3-1 & 3-2).

The difference Patterson maps were obtained with coefficient of $[F_{PH} - F_P]^2$, where PH and P stand for the heavy atom derivative and the native crystals, respectively. From the difference Patterson maps using Deriv-U and Native-III data at 5Å resolution two major binding sites of uranium atom were found, while in the corresponding maps using Deriv-Pt and Native-III data only few broad peaks were recognized. The determination of the absolute coordinations of uranium atom was performed by the difference Fourier synthesis. The phases for uranium derivative were calculated by the single isomorphous replacement method and the obtained figure of merit was 0.68 as shown in Table 3-3.

The 3Å resolution electron density maps were calculated in the form of mini-maps. Although some residues in the loop region were difficult to be traced, all residues belong to eight β–strands were

Table 3-1. *Mean Isomorphous Structure Factor Differences of the Uranium Derivative of PAZAM1*

Resolution range (Å)	No. of reflections	Average |F| of U-derivative (F1)	Average |F| of U-derivative (F2)	F1/F2	r.m.s. Δ|F|	Δ|F| / F1
10.0 - 6.01	241	12.708	12.738	0.9976	3.718	0.2925
6.01 - 4.96	229	12.996	13.306	0.9767	3.585	0.2759
4.96 - 4.39	233	17.352	17.101	1.0147	4.015	0.2314
4.39 - 4.02	236	15.304	15.318	0.9991	3.582	0.2340
4.02 - 3.75	226	14.278	14.198	1.0060	3.559	0.2492
3.75 - 3.54	223	14.019	14.146	0.9910	3.583	0.2556
3.54 - 3.37	222	13.258	13.092	1.0127	3.513	0.2649
3.37 - 3.22	204	11.851	12.430	0.9534	3.796	0.3203
3.22 - 3.10	201	10.770	10.941	0.9844	3.595	0.3338
3.10 - 3.00	199	10.317	10.708	0.9635	3.648	0.3536

Number of reflection	2214
RMS. Difference	3.663
Mean Amplitude	13.381
Fractional RMS. Difference	0.2737

Table 3-2. *Mean Isomorphous Structure Factor Differences of the Platinum Derivative of PAZAM1*

Resolution range (Å)	No. of reflections	Average |F| of U-derivative (F1)	Average |F| of U-derivative (F2)	F1/F2	r.m.s. Δ|F|	Δ|F| / F1
10.0 - 6.01	250	12.465	12.635	0.9866	1.941	0.1557
6.01 - 4.96	242	12.638	12.737	0.9938	1.729	0.1366
4.96 - 4.39	236	17.273	17.241	1.0018	1.824	0.1056
4.39 - 4.02	245	14.969	14.806	1.0010	1.949	0.1302
4.02 - 3.75	228	14.243	14.290	0.9967	1.746	0.2336
3.75 - 3.54	226	13.942	14.123	0.9872	1.620	0.1162
3.54 - 3.37	236	12.812	12.955	0.9890	1.557	0.1215
3.37 - 3.22	216	11.591	11.874	0.9762	1.733	0.1495
3.22 - 3.10	211	10.586	10.921	0.9694	1.660	0.1568
3.10 - 3.00	214	9.998	10.253	0.9751	1.596	0.1596

Number of reflection	2304
RMS. Difference	1.745
Mean Amplitude	13.117
Fractional RMS. Difference	0.1330

Table 3-3 *Heavy Atom Parameters of the Uranium Derivative*

Uranium atom site		Site 1	Site 2
Positional Parameters	X =	0.031	0.485
	Y =	0.053	0.688
	Z =	0.477	0.299
Biso (Å)		20.6	21.1
Occupancy (%)		16.6	10.1
Phase Determination			
R_K (%)		13.3	
Figure of merit		0.68	

traced easily, especially around the copper site. From the electron density maps, the copper site, the highest peak in the whole map, was analyzed to be x=0.27, y=0.26 and z=0.60, which were identical to the copper position determined in step *I* (Fig. 3-4 & 3-5).

III. Molecular replacement method

The crystal structure of PAZAM1 was finally determined by the molecular replacement method using the *MERLOT* (Fitzgerald, 1988) program package. The molecular structure of PAZS6 (Adman *et al.*, 1989) was used as the starting structure model. The atomic coordinates were obtained from the BNL protein data bank (ISSN

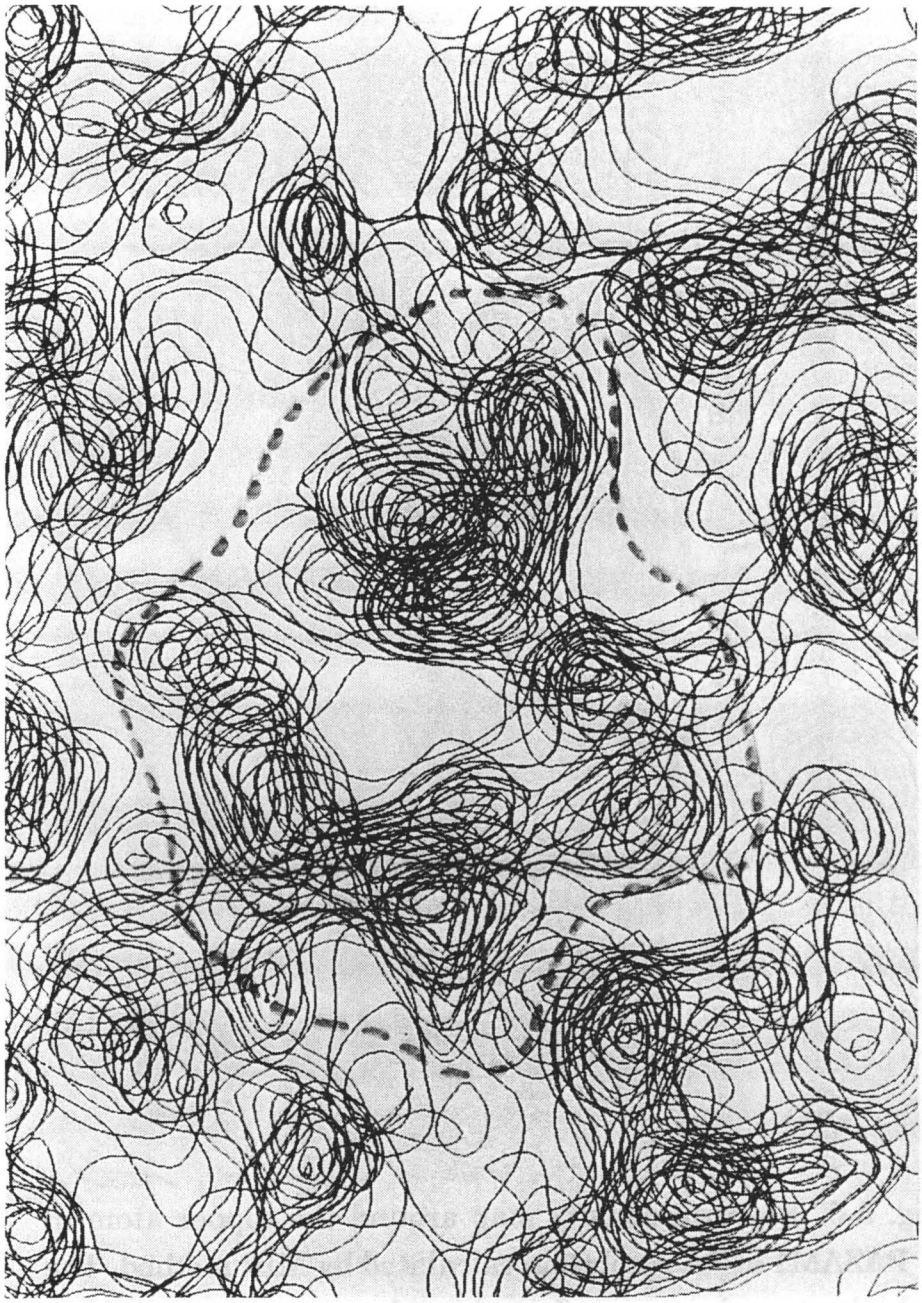

Fig. 3-4 Electron density map of PAZAM1 at 6Å resolution. one molecule of PAZAM1 (showed by a circle) was extracted for tracing.

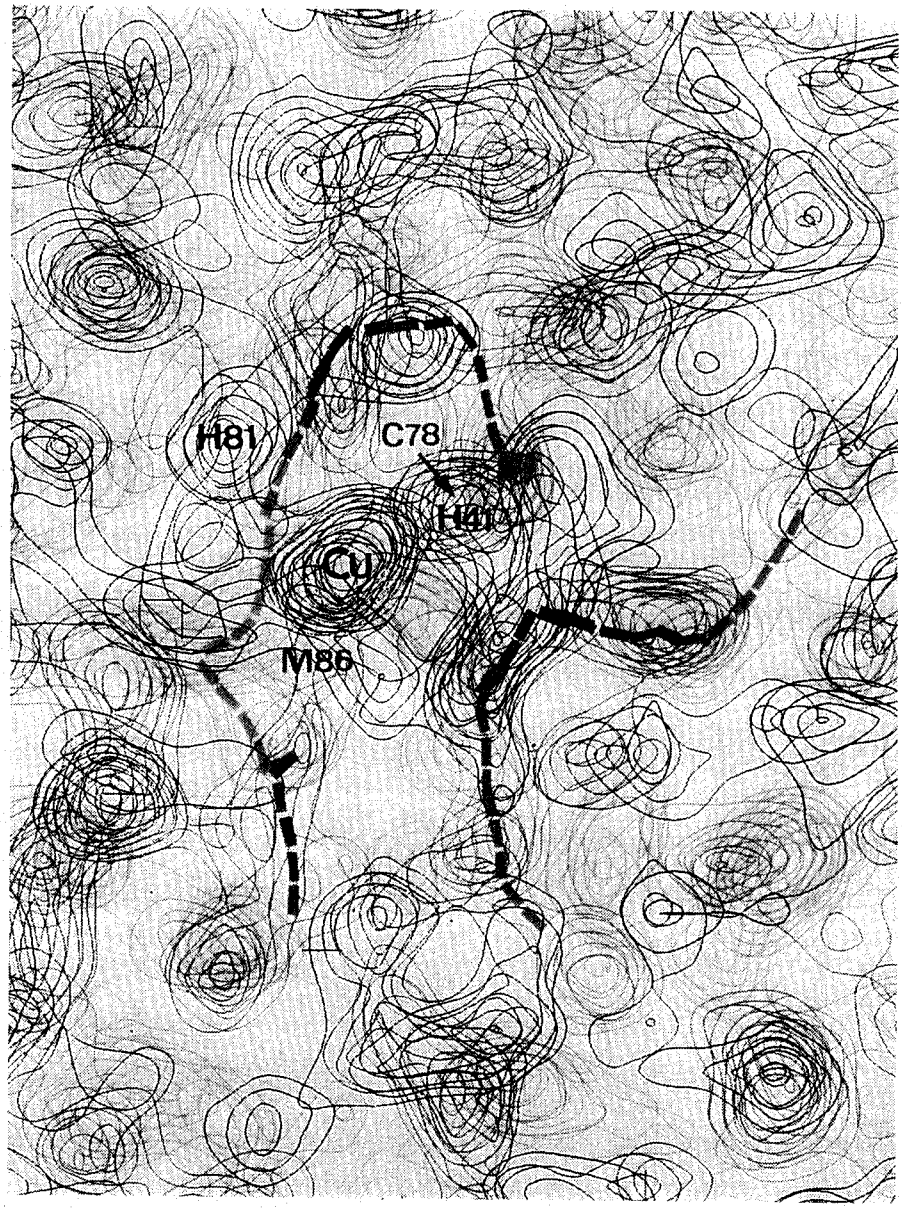

Fig. 3-5 Electron density map around the copper atom in PAZAM1 at 3Å resolution calculated by MIR method. The highest peak was confirmed as the copper atom, whose location was identical to the copper position determined by MAD method.

0021-9258). The copper atom in PAZS6 was located on an origin point of a 100 × 100 × 100 Å primitive cell and the structure factors were calculated up to 3.2Å resolution. The cross-rotation function was first calculated with the data between 13 and 3.2Å resolution in the *CROSUM* (Crowther, 1972) function and each set of rotation parameters thus obtained were sequentially used to calculate *R*-value in the *RMINIM* (Ward *et al.*, 1975) function. In the *RMINIM* calculations the molecular translational parameters were fixed to the position of copper atom in PAZAM1 which was independently obtained by MIR and MAD method. The 12th highest peak (α=45.0, β=76.0, γ=195.0) and the translation parameters yield a minimum *R*-factor after 5 cycles of minimizations in *RMINIM* function. The rotational parameters are dependent on the resolution range used in the calculation. When the data between 13.0Å and 3.2Å resolution was used in the rotation calculations, the correct peak was found in the 5th peak with the hight of 82% against the highest peak and 4.4s (Table 3-4 and 3-5).

After several cycles of subsequent refinement, the best positional parameters gave the *R*-factor of 53.9%; the final Eular angles were α=48.80, β=77.61, γ=193.89 and the final translation parameters were x=0.2814, y=0.2620, z=0.5944. The initial atomic

Table 3-4. *Results of rotation function and R-factor calculation for PAZAM1*

Peak ranking	rotation angle α	β	γ	peak height	sigma (σ)	*R*-factor (%)
1	75.00	58.00	170.00	100.00	5.27	76.5
2	67.50	80.00	185.00	92.89	4.90	73.8
3	162.50	59.00	165.00	81.66	4.30	70.9
4	120.00	46.00	210.00	77.61	4.09	84.4
5	60.00	37.00	175.00	74.84	3.94	76.0
6	60.00	25.00	250.00	73.79	3.89	77.2
7	95.00	35.00	135.00	73.32	3.86	78.7
8	55.00	25.00	255.00	70.59	3.72	77.3
9	2.50	40.00	130.00	69.74	3.67	73.5
10	172.50	20.00	330.00	69.70	3.67	73.3
11	167.50	20.00	335.00	69.35	3.65	86.4
12	45.00	76.00	195.00	67.63	3.56	61.4
13	105.00	80.00	315.00	66.87	3.52	75.3
14	100.00	31.00	130.00	66.72	3.51	75.3
15	177.50	50.00	135.00	66.71	3.51	75.7
16	125.00	37.00	100.00	66.65	3.51	74.6
17	175.00	52.00	140.00	66.50	3.50	72.5
18	45.00	83.00	350.00	66.45	3.50	66.9
19	20.00	45.00	155.00	66.35	3.49	72.7
20	45.00	89.00	335.00	65.91	3.47	74.2
21	140.00	38.00	130.00	65.67	3.46	72.7
22	177.50	41.00	135.00	65.48	3.45	73.9
23	160.00	19.00	340.00	65.01	3.42	75.5

Table 3-5. *The dependence of the correct rotation peak on the resolution for PAZAM1*

Reso. range (Å)		Sigma cut	Correct peak ranking			First incorrect peak ranking		
R_{max}	R_{min}		Rank	Height(%)	Height(σ)	Rank	Height(%)	Height(σ)
7.0 -	3.2	3.0	13	66.78	3.52	1	100	5.28
7.0 -	4.0	3.0	16	75.15	3.24	1	100	3.24
7.0 -	5.0	3.0	-	-	-	1	100	3.69
8.0 -	3.2	3.0	13	69.83	3.59	1	100	5.15
9.0 -	3.2	3.0	8	71.97	3.67	1	100	5.12
10.0 -	3.2	3.0	8	72.57	3.64	1	100	5.05
11.0 -	3.2	3.0	6	72.06	3.81	1	100	5.30
12.0 -	3.2	3.0	5	68.40	3.72	1	100	5.42
13.0 -	3.2	3.0	5	81.84	4.37	1	100	5.32
14.0 -	3.2	3.0	4	74.55	4.08	1	100	5.44
15.0 -	3.2	3.0	4	77.66	4.14	1	100	5.31
16.0 -	3.2	3.0	4	82.26	4.14	1	100	5.01
17.0 -	3.2	3.0	4	82.78	4.03	1	100	4.85
18.0 -	3.2	3.0	4	86.39	3.91	1	100	4.50
19.0 -	3.2	3.0	4	88.81	3.88	1	100	4.35
20.0 -	3.2	3.0	4	80.24	3.80	1	100	4.72

coordinates for current structure were generated by using these parameters in the *ROTTRN* function.

3-1-2 Molecular Replacement Method for Analyzing of PAZIAM

The molecular structure of PAZS6 was also used as the starting model for structure analysis of PAZIAM. The ratios of identical *vs.* total residues are 81/123 (66%) for PAZIAM-PAZS6.

The rotation search was carried out in the range of 0-180, 0-90 and 0-360 for Eulerian angles of α, β and γ. The translation parameters were calculated in the *RVAMAP* function for each rotation peak. Thus, the rotation and translation parameters are calculated and the *R*-factor was calculated for each case and the minimum *R*-factors are listed in Table 3-6. The correct rotation peak was found at 1st Eulerian angles of α=115.0°, β=60.0° and γ=305.0° for 13-3.2Å resolution data, and the translation parameters of x=0.45, y=0.10 and y=0.15 in fraction of unit cell gave the minimum *R*-factor of 64.9% for 15-3.88Å resolution data (Table 3-7).

After several cycles of the *RMINIM* function (Ward, 1975), the rotation parameters converged to α=115.40°, β=62.23° and γ=303.99°, and the translation parameters to x=0.4537, y=0.1330 and z=0.1387. The *R*-factor calculated for the model structure was 47.5% for 15.0-3.88Å data.

Table 3-6 *Results of Rotation function for PAZIAM*

Conditions: Resolution range (Å) 13.0 - 3.2
Cut off radius (Å) 19.1
Sigma cut 2.0

α	β	γ	peak height	sigma
115.00	60.00	305.00	100.00	4.83
10.00	38.00	45.00	86.44	4.18
170.00	83.00	275.00	74.02	3.57
15.00	23.00	200.00	72.19	3.49
32.50	40.00	130.00	70.73	3.42
145.00	73.00	265.00	69.77	3.37
150.00	53.00	345.00	68.46	3.31
5.00	87.00	230.00	67.35	3.25
150.00	52.00	310.00	66.81	3.23
17.50	61.00	85.00	65.16	3.15

Table 3-7 *Results of Translation function for PAZIAM by RVAMAP Function*

Conditions: Resolution range (Å) 15.0 - 3.88
Sigma cut 2.0

a	b	c	peak height	sigma	R-factor
45.00	10.00	15.00	100.00	3.59	0.649
45.00	30.00	15.00	97.18	3.23	0.659
45.00	40.00	15.00	94.56	2.89	0.668
30.00	35.00	35.00	91.90	2.56	0.677
20.00	40.00	0.00	91.37	2.49	0.679
20.00	20.00	0.00	91.01	2.44	0.680
40.00	35.00	35.00	90.95	2.44	0.681
45.00	40.00	0.00	90.33	2.36	0.683
20.00	20.00	15.00	89.81	2.29	0.685
45.00	25.00	0.00	89.48	2.25	0.686

3-1-3 Molecular Replacement Method for Analyzing of AZUNCIB

The molecular structures of azurins from *alcaligenes denitrificans* NCTC8582 and *pseudomonas aeruginosa* were revealed at 1.8Å and 3.0Å, respectively (Baker, 1987, AZUNCTC)(Adman, 1978, AZUAER).

The ratios of identical *vs.* total residues are 90/129 (70%) for both AZUNCIB-AZUNCTC and AZUNCIB-AZUAER. Because the AZUNCTC is analyzed at higher resolution, it was used as the starting model. The ranges of rotation search are set as 0-90°, 0-90° and 0-360° for Eulerian angles of α, β and γ and the increments of search are set as 1.25° 1.00° and 5.00°, respectively. The translation parameters were calculated in the *RVAMAP* function for each rotation peak. Thus, the rotation and translation parameters are calculated and the *R*-factor was calculated for each case and the minimum *R*-factors are listed in Table 3-8. The correct rotation peak was found at 13th Eulerian angles of α=88.75°, β=2.00° and γ=310.0° for 15-3.2Å resolution data, and the translation parameters of x=0.15, y=0.20 and y=0.00 in fraction of unit cell gave the minimum *R*-factor of 47.1% for 15-3.88Å resolution data.

After several cycles of the *RMINIM* function (Ward, 1975), the rotation parameters converged to α=90.65°, β=0.20° and γ=311.90°, and the translation parameters to x=0.137, y=0.179 and z=0.002. The

R-factor calculated for the model structure was 35.4% for 15.0-3.88Å data.

Table 3-8 *Results of Rotation function for AZUNCIB*

Conditions: Resolution range (Å) 15.0 - 3.2
Cut off radius (Å) 19.18
Sigma cut 2.0

α	β	γ	peak height	sigma	*R*-factor
28.75	3.00	280.00	100.00	3.56	72.6
23.75	3.00	285.00	99.94	3.56	67.4
33.75	3.00	275.00	99.90	3.56	67.7
18.75	3.00	290.00	99.72	3.55	67.5
38.75	3.00	270.00	99.65	3.55	67.8
13.75	3.00	295.00	99.35	3.54	67.6
43.75	3.00	265.00	99.26	3.54	68.1
48.75	2.00	260.00	98.89	3.52	64.5
8.75	3.00	300.00	98.82	3.52	67.7
53.75	2.00	255.00	98.50	3.51	61.0
3.75	2.00	305.00	98.30	3.50	68.0
58.75	2.00	250.00	98.03	3.49	66.2
88.75	2.00	310.00	97.78	3.48	47.1
63.75	2.00	245.00	97.49	3.47	60.9
0.00	2.00	310.00	97.25	3.46	65.6

3-2 Refinement Protocol

Refinements of the crystal structures of three blue copper proteins were carried out using both stereochemically restrained least-squares refinement method (*PROLSQ*; Hendrickson, 1981) and the simulated annealing refinement method containing molecular dynamics optimization (*X-PLOR*; Brünger, 1987). The refinements were carried out on the NEC EWS 4800/220 for *PROLSQ* and on the IRIS 4D 25GT for *X-PLOR*. Model building was performed on IRIS using the program *FRODO* (Jones, 1978). Both $2F_O$-F_C and difference Fourier maps as well as omit maps were used throughout.

The first step of the refinement was performed using *X-PLOR* ver. 2.2 (Brünger, 1990). Because of the ambiguity for the energy constraint parameters of metal atom used in the molecular dynamics refinement, a somewhat unreliable copper geometries were obtained for each case. In order to obtain exact copper geometries no restraint was imposed on the copper coordination through the final stage of refinement by *PROLSQ*.

Water molecules were added in some separate steps by the use of *PEAK* program (Okamoto & Hirotsu, unpublished) to select peaks on the F_O-F_C maps followed by the program *WATER* (Okamoto & Hirotsu, unpublished) to assign water molecules to the peaks with

reasonable distances for both water-protein and water-water interactions.

3-2-1 Refinement of PAZAM1

By using prepstage refinement, *R*-factor decreased from 51.6% to 33.3% with 2.5Å resolution data, and by simulated annealing calculation at 3000K, *R*-factor became 23.9% in the range from 5 to 2.5Å resolution data. The resulted $2F_O$-F_C electron density map were continuous except the C-terminal residue. Then further 3 steps of refinement were performed by *X-PLOR* using the stepwisely increased data. Consequently, the refinement of molecular dynamics brought *R*-factor of 26.0% with data up to 2.0Å. The results of the slow-cooling refinement by *X-PLOR* were summarized in Table 3-9.

Table 3-10 shows the results of seven stages of the refinement process by *PROLSQ*. Every stage includes model improvement followed by several cycles of refinement. Model improvement was carried out based on the Fourier maps calculated with the coefficients of $(2F_O\text{-}F_C)\exp(2\text{pia}_{\text{calc}})$ and $(F_O\text{-}F_C)\exp(2\text{pia}_{\text{calc}})$.

Total of 132 water molecules were included in the final structure model and further rebuilding and cycles of refinement for the water structure finally decreased *R*-factor to 19.9% for 1.5Å resolution.

Table 3-9 *Results of the refinement of PAZAM1 by X-PLOR*

Step	Resolution range (Å)	CHECK	PREPSTGE	SLOWCOOL
1	5.0 - 2.5	51.6%	33.3%	3000K 23.9%
2	5.0 - 2.5	38.8%	24.3%	4000K 23.6%
3	5.0 - 2.0	40.4%	28.4%	4000K 26.6%
4	5.0 - 2.0	39.6%	27.1%	4000K 26.0%

Table 3-10 *Results of the refinement of PAZAM1 by PROLSQ*

Resolution range (Å)	No. of atoms	No. of parameters	No. of waters	No. of reflections	No. of cycles	*R* -factor initial	final
5.0 - 2.0	938	3753	0	9250	12	25.9	22.5
5.0 - 1.8	938	3753	0	9601	4	25.7	22.9
5.0 - 1.5	938	3753	0	13710	4	27.6	24.6
8.0 - 1.5	938	3753	0	14365	10	29.1	26.6
8.0 - 1.5	999	3997	61	14365	10	28.6	23.3
8.0 - 1.5	1052	4209	114	14365	13	27.2	22.0
8.0 - 1.5	1070	4281	132	14365	12	26.7	19.9

3-2-2 Refinement of PAZIAM

After correction of the sequence differences between PAZS6 and PAZIAM, the refinement of the crystal structure was carried out against 3.0Å data by application of the energy-restrained minimization procedure of *X-PLOR*. After one cycle of slow-cooling refinement, the crystallographic *R*-factor decreased from 47.5% to 17.5%. Then further 1 more step of refinement were performed by *X-PLOR*. Consequently, the refinement of molecular dynamics brought *R*-factor of 22.5% with data up to 2.5Å. The results of the slow-cooling refinement by *X-PLOR* were summarized in Table 3-11.

Table 3-12 shows the results of seven stages of the refinement process by *PROLSQ*. Every stage includes model improvement followed by several cycles of refinement. Model improvement was carried out based on the Fourier maps calculated with the coefficients of $(2F_O\text{-}F_C)\exp(2\text{pia}_{\text{calc}})$ and $(F_O\text{-}F_C)\exp(2\text{pia}_{\text{calc}})$.

Total of 147 water molecules were included in the final structure model and further rebuilding and cycles of refinement for the water structure finally decreased *R*-factor to 19.2% for 1.8Å resolution.

Table 3-11 *Results of the refinement of PAZIAM by X-PLOR*

Step	Resolution range (Å)	CHECK	PREPSTGE	SLOWCOOL
1	5.0 - 3.0	47.5%	25.6%	4000K 17.5%
2	5.0 - 2.5	38.6%	22.5%	4000K 20.1%

Table 3-12 *Results of the refinement of PAZIAM by PROLSQ*

Resolution range (Å)	No. of atoms	No. of parameters	No. of waters	No. of reflections	No. of cycles	*R* -factor initial	final
10.0 - 2.5	985	3941	63	3134	15	20.0	17.3
10.0 - 2.5	985	3941	63	3134	15	20.1	18.4
10.0 - 2.2	985	4173	63	4820	30	24.7	21.4
10.0 - 2.2	1007	4029	87	4820	30	20.1	17.9
10.0 - 2.0	1007	4029	87	6533	10	20.3	19.5
10.0 - 1.9	999	3997	79	7627	10	20.8	20.9
10.0 - 1.8	1070	4281	147	9995	15	20.9	19.2

3-2-3 Refinement of AZUNCIB

By using prepstage refinement, *R*-factor decreased from 44.4% to 23.8% with 3.0Å resolution data, and by simulated annealing calculation at 3000K, *R*-factor became 19.6% in the range from 6 to

3.0Å resolution data. 1 more step of refinement was performed, the crystallographic *R*-factor decrease to 23.2% with data up to 2.5Å. The results of the slow-cooling refinement by *X-PLOR* were summarized in Table 3-13

Table 3-14 shows the results of two stages of the refinement process by *PROLSQ*. Each stage includes model improvement followed by several cycles of refinement. Model improvement was carried out based on the Fourier maps calculated with the coefficients of $(2F_O\text{-}F_C)\exp(2\pi i\alpha_{calc})$ and $(F_O\text{-}F_C)\exp(2\pi i\alpha_{calc})$.

Table 3-13 *Results of the refinement of AZUNCIB by X-PLOR*

Step	Resolution range (Å)	CHECK	PREPSTGE	SLOWCOOL	
1	6.0 - 3.0	44.4%	23.8%	3000K	19.6%
2	6.0 - 2.5	38.3%	25.2%	3000K	23.2%

Table 3-14 *Results of the refinement of AZUNCIB by PROLSQ*

Resolution range (Å)	No. of atoms	No. of parameters	No. of waters	No. of reflections	No. of cycles	R -factor initial	R -factor final
5.0 - 2.5	978	2936	0	4250	11	23.9	23.5
5.0 - 2.5	978	2936	0	4536	8	23.5	23.0
6.0 - 2.5	1043	4173	65	4536	8	22.2	20.5

Total of 65 water molecules were included in the present model and further rebuilding and cycles of refinement for the water structure at present decreased R-factor to 20.5% for 2.5Å resolution.

3-3 Refinement summary

3-3-1 Refinement Summary of PAZAM1

The refined crystal structure includes 1070 protein atoms (non-hydrogen), one metal ion and 132 water molecules. The last cycle of the refinement with 14365 unique reflections in the range of 8.0 and 1.5Å resolution gave the crystallographic *R*-factor of 19.9% with quite reasonable stereochemistry. The root-mean-square (r.m.s.) deviations from standard values are 0.024Å in bond distances (1-2 distance), 0.039Å in angle distances (1-3 distance) and 0.044Å in dihedral angles (planar 1-4 distance). Table 3-15 gives the final refinement statistics. A Ramachandran plot is given in Fig. 3-4. Because there are few residues outside the allowed regions, the current model is considered to have a good stereochemistry. The r.m.s. error of the atomic positions estimated by the Luzzati plot (Luzzati, 1952) is between 0.10 and 0.15Å, but the structure of the copper site is so rigid and its electron density is so clear that the error may be much less for the copper coordination geometry.

3-3-2 Refinement Summary of PAZIAM

The refined crystal structure includes 1070 protein atoms (non-hydrogen), one metal ion and 147 water molecules. The last

Table 3-15. *Final refinement statistics for PAZAM1*

Resolution range(Å)	8.0 - 1.5
Number of reflections	14,365
Completeness (8.0 - 1.5Å)	75.5
Total number of atoms (non-hydrogen)	1,070
Solvent atoms (non-hydrogen)	132
R-factor (8-1.5Å)	19.9%
Average B-factors ($Å^2$)	
Main-chain	12.9
Side-chain	13.8
Solvent	32.4
Root-mean square deviation from standard values	
Bonds (1-2 distance) (Å)	0.024
Angles (1-3 distance) (Å)	0.039
Dihedral angles (1-4 distance) (Å)	0.044

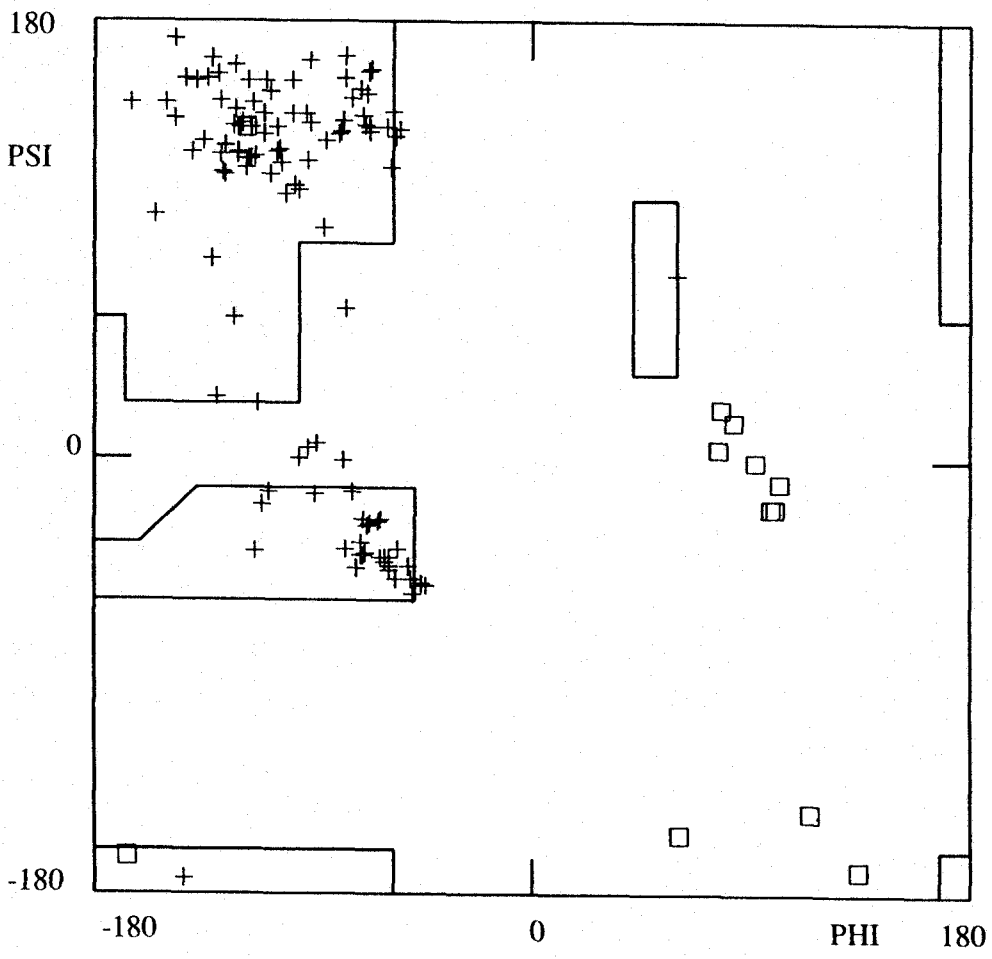

Fig. 3-6 Ramachandran plot of the final model of PAZAM1. Glycine residues are marked with squares.

cycle of the refinement with 8995 unique reflections in the range of 10.0 and 1.8Å resolution gave the crystallographic *R*-factor of 19.2% with quite reasonable stereochemistry. The root-mean-square (r.m.s.) deviations from standard values are 0.018Å in bond distances (1-2 distance), 0.029Å in angle distances (1-3 distance) and 0.032Å in dihedral angles (planar 1-4 distance). Table 3-16 gives the final refinement statistics. A Ramachandran plot is given in Fig. 3-5.

3-3-3 Refinement Summary of AZUNCIB

The refined crystal structure includes 1043 protein atoms (non-hydrogen), one metal ion and 65 water molecules. The last cycle of the refinement with 4536 unique reflections in the range of 6.0 and 2.5Å resolution gave the crystallographic *R*-factor of 20.5% with quite reasonable stereochemistry. The root-mean-square (r.m.s.) deviations from standard values are 0.017Å in bond distances (1-2 distance), 0.033Å in angle distances (1-3 distance) and 0.034Å in dihedral angles (planar 1-4 distance). Table 3-17 gives the final refinement statistics. A Ramachandran plot is given in Fig. 3-6. Because there are few residues outside the allowed regions, the current model is considered to have a good stereochemistry.

Table 3-16. *Final refinement statistics for PAZIAM*

Resolution range(Å)	10.0 - 1.8
Number of reflections	8995
Completeness (10.0 - 1.5Å)	0.85
Total number of atoms (non-hydrogen)	1,070
Solvent atoms (non-hydrogen)	147
R-factor (8-1.5Å)	19.2%
Root-mean square deviation from standard values	
Bonds (1-2 distance) (Å)	0.018 (0.030)
Angles (1-3 distance) (Å)	0.029 (0.040)
Dihedral angles (1-4 distance) (Å)	0.032 (0.050)

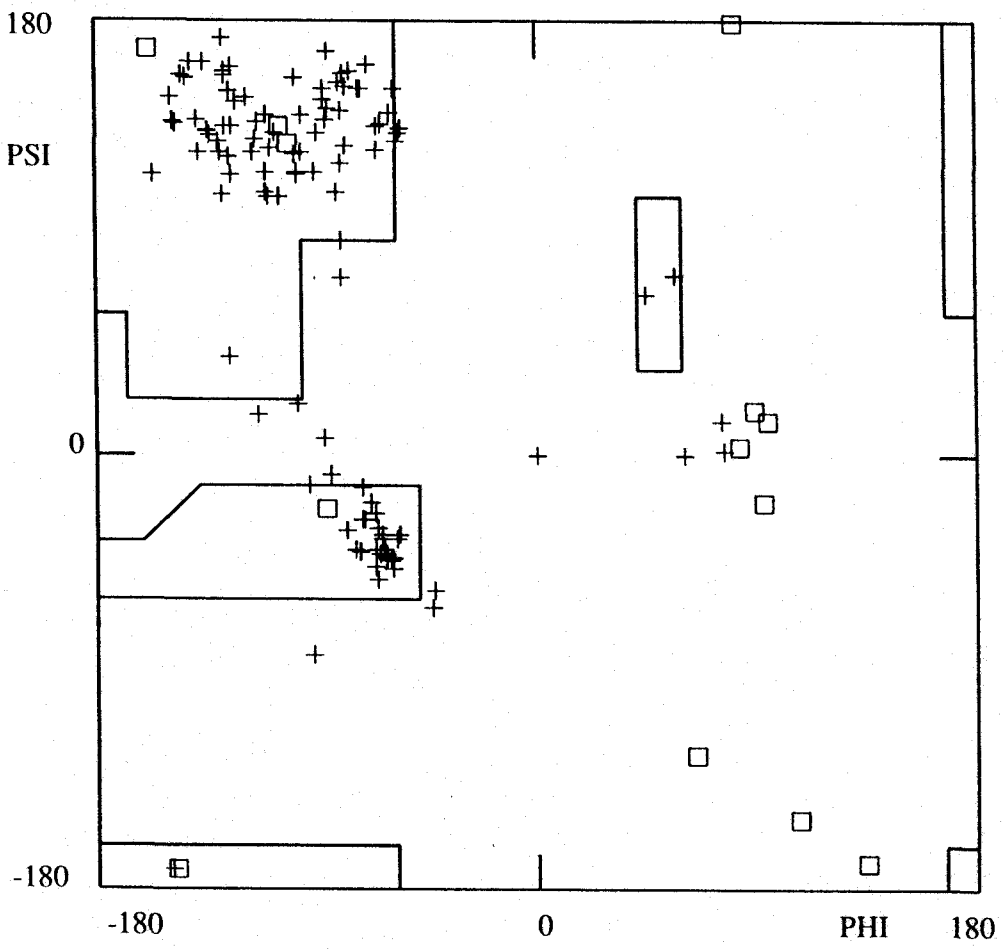

Fig. 3-7 Ramachandran plot of the final model of PAZIAM. Glycine residues are marked with squares.

Table 3-17. *Final refinement statistics for AZUNCIB*

Resolution range(Å)	6.0 - 2.5
Number of reflections	4536
Completeness (6.0 - 2.5Å)	0.53
Total number of atoms (non-hydrogen)	1,043
Solvent atoms (non-hydrogen)	65
R-factor (6-2.5Å)	20.5%
Root-mean square deviation from standard values	
Bonds (1-2 distance) (Å)	0.017 (0.030)
Angles (1-3 distance) (Å)	0.033 (0.040)
Dihedral angles (1-4 distance) (Å)	0.034 (0.050)

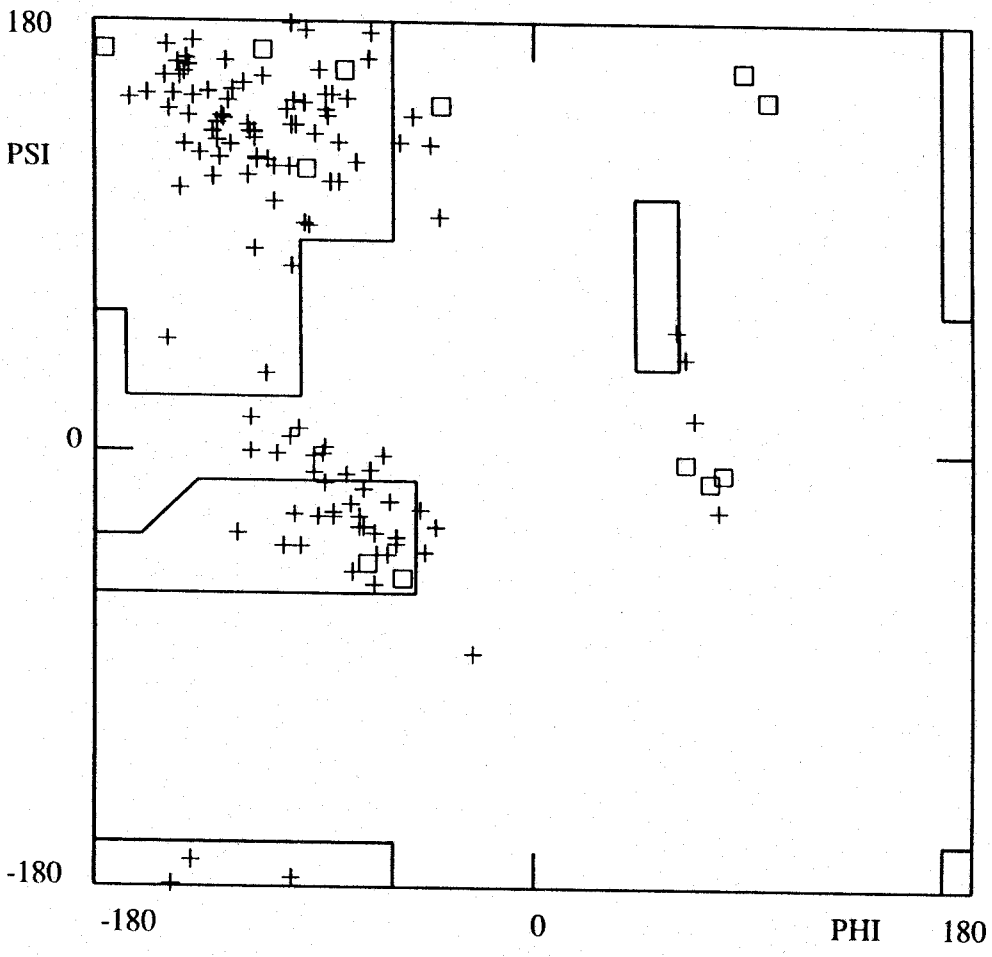

Fig. 3-8 Ramachandran plot of the final model of AZUNCIB. Glycine residues are marked with squares.

4 Obtained Structures and Comparison of Blue Copper Proteins

4-1 Molecular Structures of PAZAM1 and PAZIAM

The complete models for all nonhydrogen atoms of PAZAM1 and PAZIAM, excluding water molecules, are shown in Fig. 4-1 and Fig. 4-2. The backbone structures and the schematic models are also shown. Both pseudoazurin molecules are approximately spherical and have overall dimensions of $38 \times 38 \times 27$ $Å^3$, which is almost the same size of PAZS6 used as the starting structural model in the molecular replacement method. Both molecules have β–barrel structures formed by eight strands and topological structures of them are same (Fig. 4-3). For the structure of PAZAM1, each strand consists of 5 to 11 residues: I, 1-8; II, 17-27; III, 29-34; IV, 40-46; V, 53-59; VI, 62-70; VII, 73-77; VIII, 87-92. Residues 97-108 and 111-123 make two α–helices. The β–barrel is built up by two β–sheets; one is formed by strands I, II, III, and VI and the other is formed by strands IV, V, VII, and VIII. The topology of 'Greek key' , which is generally accepted in the protein formed by β–barrel, is also found when the barrel is opened between the strand II and VIII. Those features are also found in the structure of PAZIAM.

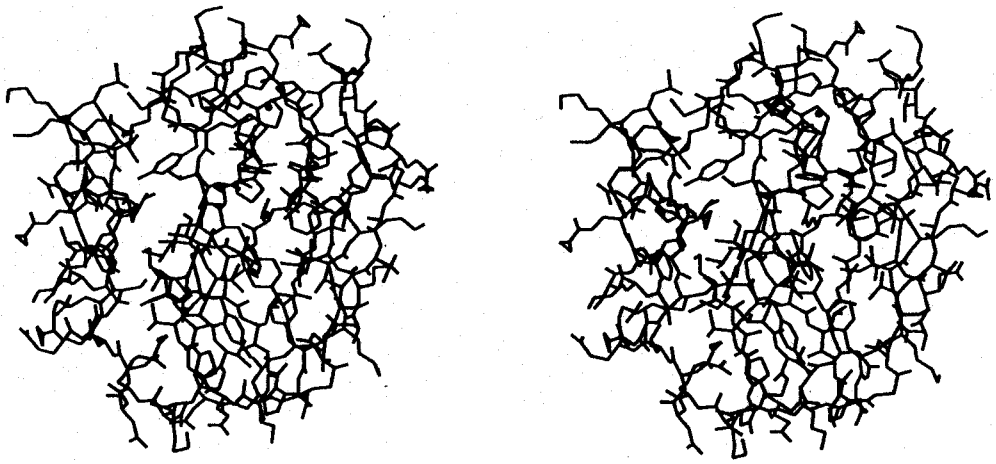

(a)

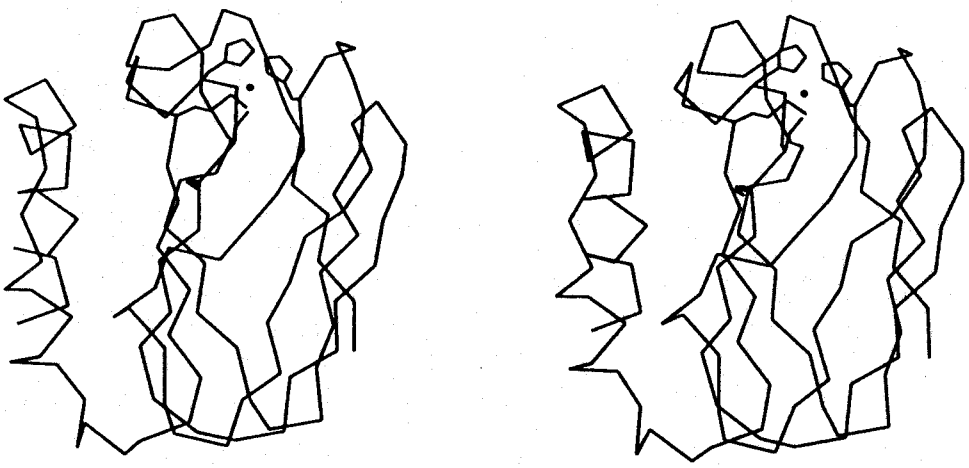

(b)

Fig. 4-1 Stereoviews of the overall structure of PAZAM1. (a) All the nonhydrogen atoms excluding water molecules, (b) mainchain structure of pseudoazurin, are shown together with the copper atom by a plot and (c) schematic drawing of PAZAM1 by MOLSCRIPT (next page).

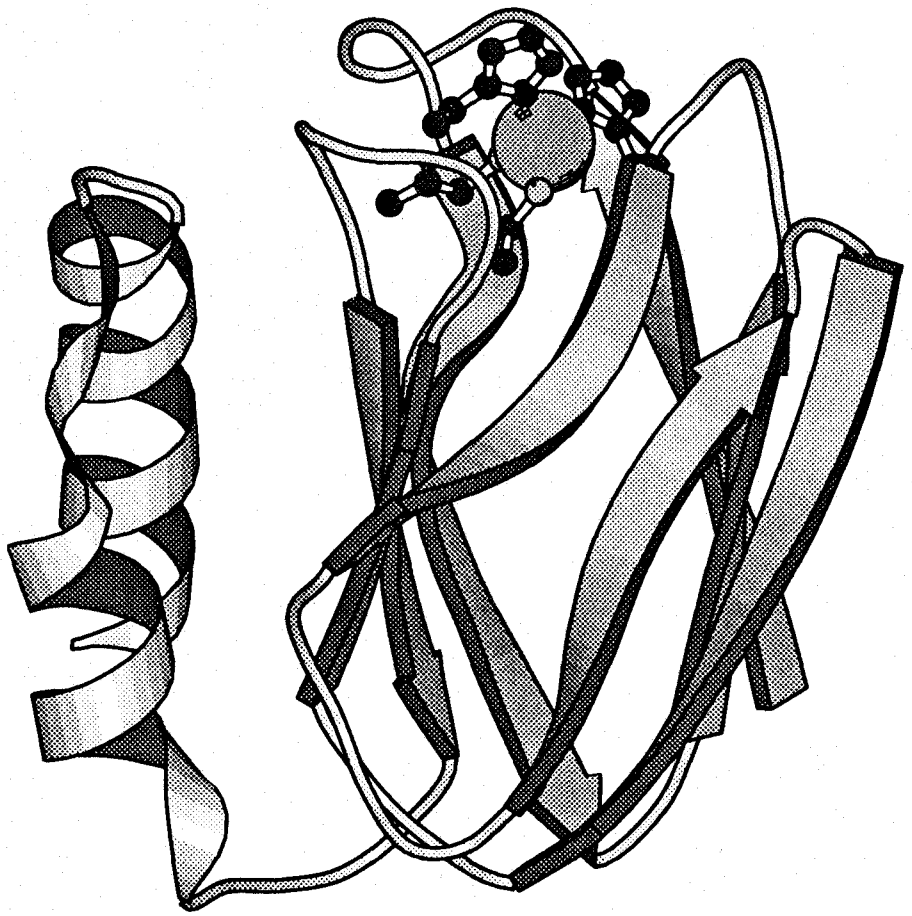

Fig. 4-1 (c) Schematic drawing of PAZAM1

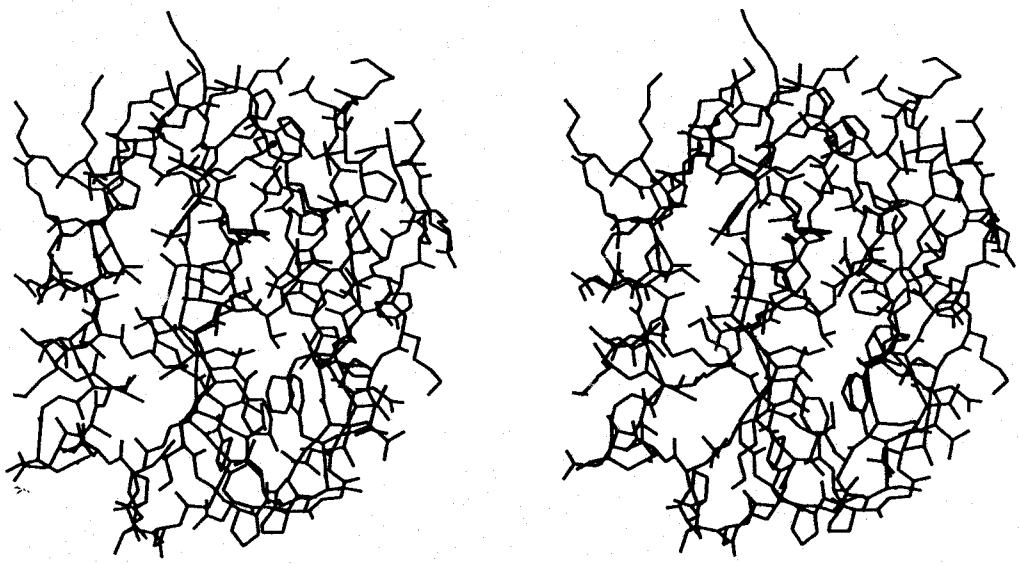

(a)

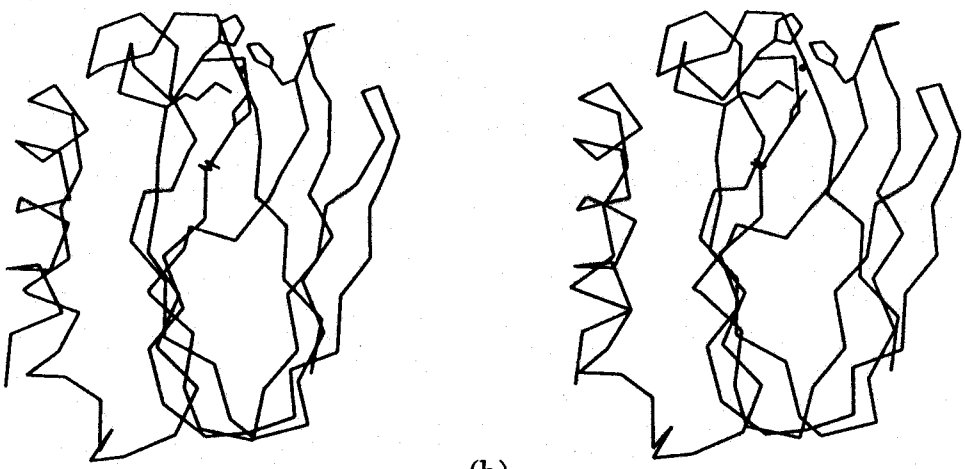

(b)

Fig. 4-2 Stereoviews of the overall structure of PAZIAM. (a) All the nonhydrogen atoms excluding water molecules, (b) mainchain structure of pseudoazurin, are shown together with the copper atom by a plot and (c) schematic drawing of PAZIAM by MOLSCRIPT (next page).

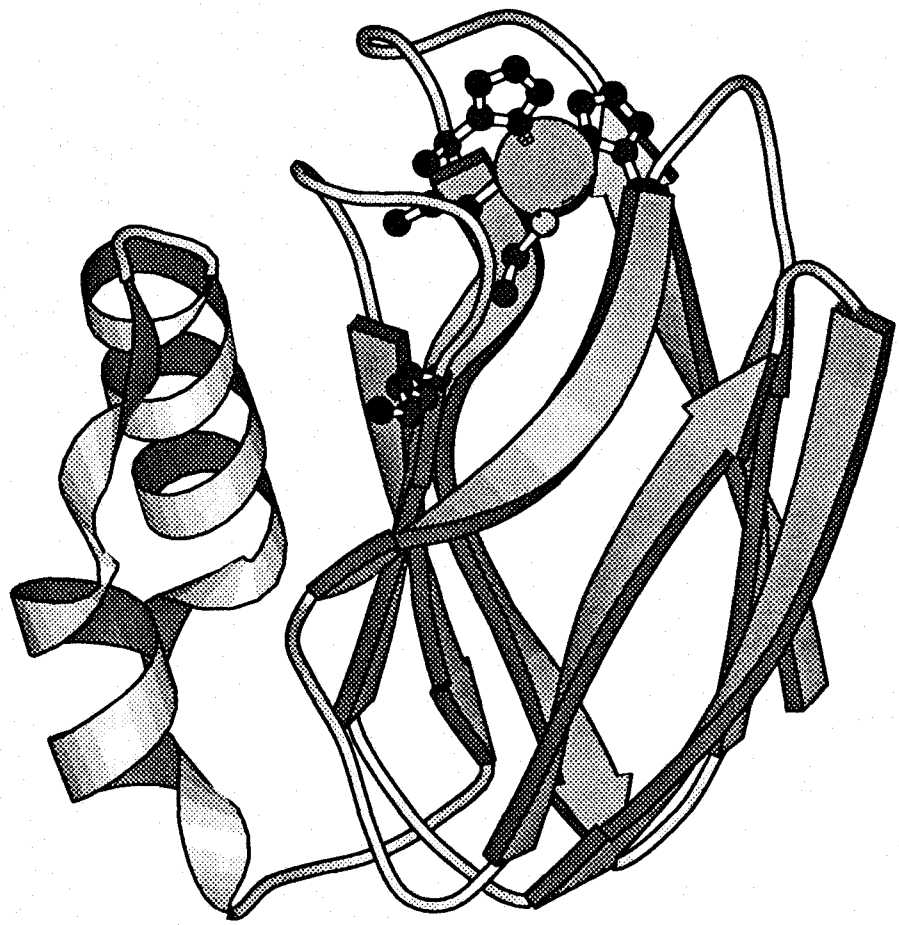

Fig. 4-2 (c) Schematic drawing of PAZIAM

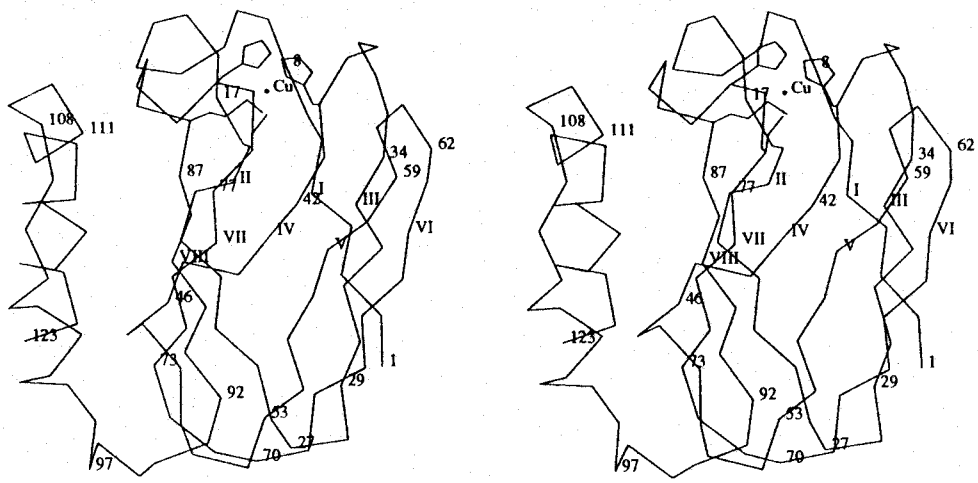

Fig. 4-3 A stereoview of the topological structure of PAZAM1. The overall structure is an eight-stranded b-barrel that forms two b-sheets. One is composed of strands I, II, III and VI, and the other is consisted by strands IV, V, VII and VIII. The copper atom shown by a dot is located at the northern end of the molecule.

The locations of copper atoms are the northern end of the molecules and the four amino acids ligating to the copper atoms are also conserved in three pseudoazurins.

The 'kink' structure in the strand II, which is peculiar to the starting model of PAZS6, is also confirmed in the electron density maps with the coefficient of $2F_O$-F_C and also in the omit maps of both molecular structures. This structure contains a dislocation in the middle of the β–strand II, but the gap is stabilized by the hydrogen bonds between the strands I and II or the strands II and VIII.

In those ways, the molecular structures of PAZAM1 and PAZIAM are found to be similar to that of PAZS6 used as the starting model in the structure analysis. It is reasonable that the overall structures are very similar because of the high homologies among three pseudoazurins. The proportions of identical residues are 54/123 (44%) for PAZAM1-PAZS6, 81/123 (66%) for PAZIAM-PAZS6 and 64/123(52%) for PAZAM1-PAZIAM. Then, the superimposed structures were calculated using the program of MIDASPLUS (Ferrin, 1988). Fig. 4-4 shows the superimposed structures of PAZAM1 and PAZS6. Those pseudoazurins are so analogous that a very small value of 1.42Å was calculated as the averaged r.m.s. deviations for all backbone atoms of AM1-S6. In the same way, 1.13Å and 1.67Å were obtained for backbone structures of IAM-S6 and

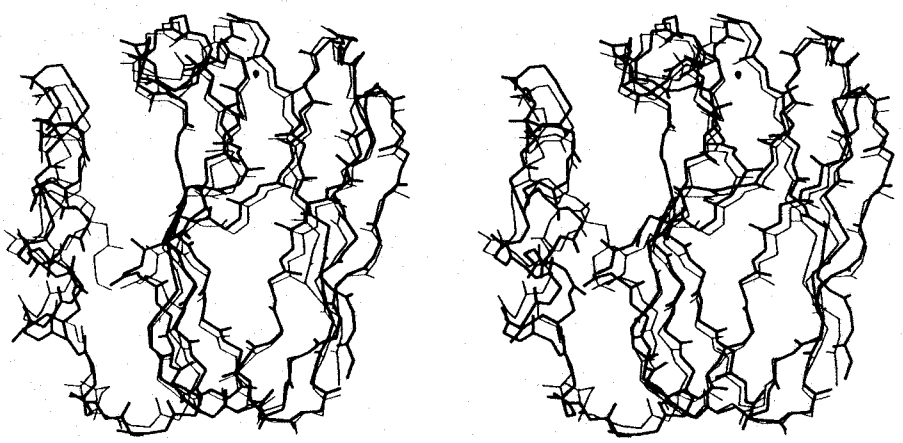

Fig 4-4 Stereo view of the backbone structures of PAZAM1 and PAZS6 superimposed. PAZAM1 is shown with thick lines, PAZS6 with thin lines. Total of 740 atoms were matched (370 atoms for PAZAM1 and 370 atoms for PAZS6) and r.m.s. error is 1.41Å.

Table 4-1 *R.M.S. Differences among Three Pseudoazurins*

	AM1-S6	IAM-S6	AM1-IAM
No. of homologous sequences	54(123)	81(123)	64(123)
Sequences homology (%)	44	66	52
No. of atoms for the calculation	369	369	370
R.M.S. difference (Å)	1.42	1.13	1.67

AM1-IAM, respectively (Table 4-1). These small parameters show definitely that the overall structures of three pseudoazurins are conserved.

4-2 Molecular Structures of AZUNCIB

The complete models for all nonhydrogen atoms of AZUNCIB, excluding water molecules, are shown in Fig. 4-5. The backbone structures and the schematic models are also shown. The whole structural features found in AZUNCIB are common to those had been accepted in the blue copper proteins. The basic folding of the azurin molecule is also a β–barrel structure like pseudoazurin or

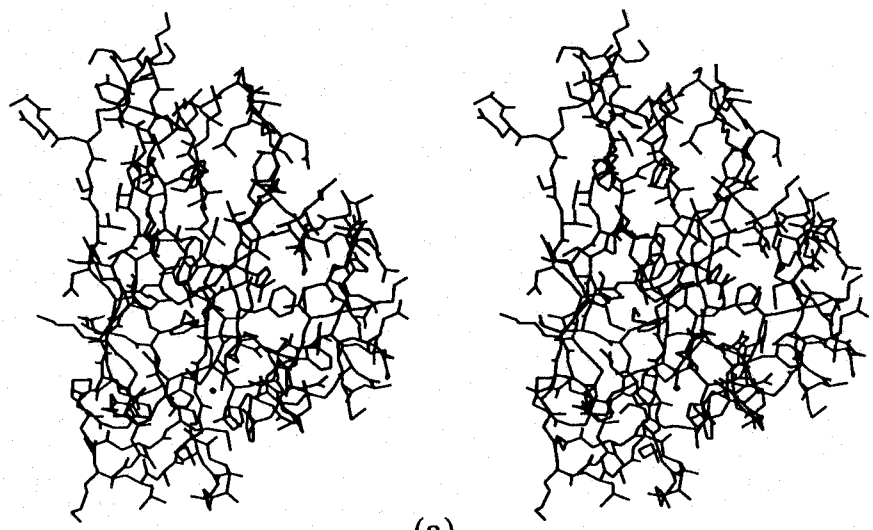

(a)

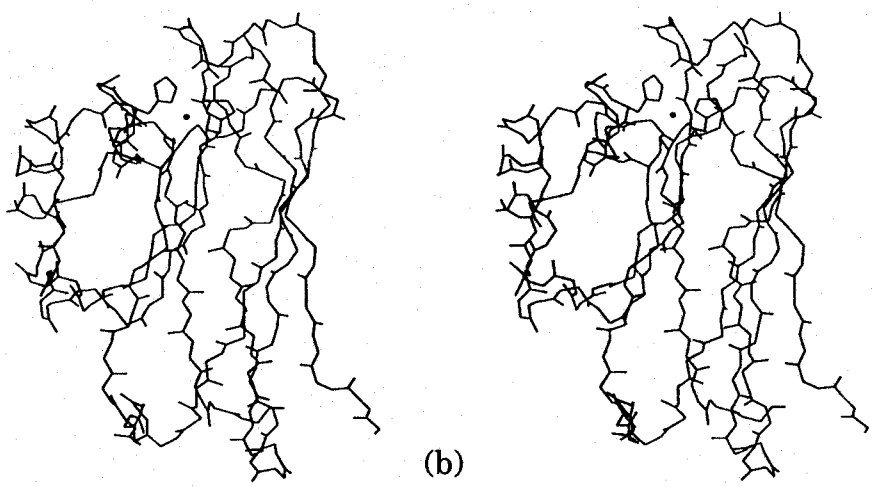

(b)

Fig. 4-5 Stereoviews of the overall structure of AZUNCIB. (a) All the nonhydrogen atoms excluding water molecules, (b) mainchain structure of azurin, are shown together with the copper atom by a plot and (c) schematic drawing of AZUNCIB by MOLSCRIPT (next page).

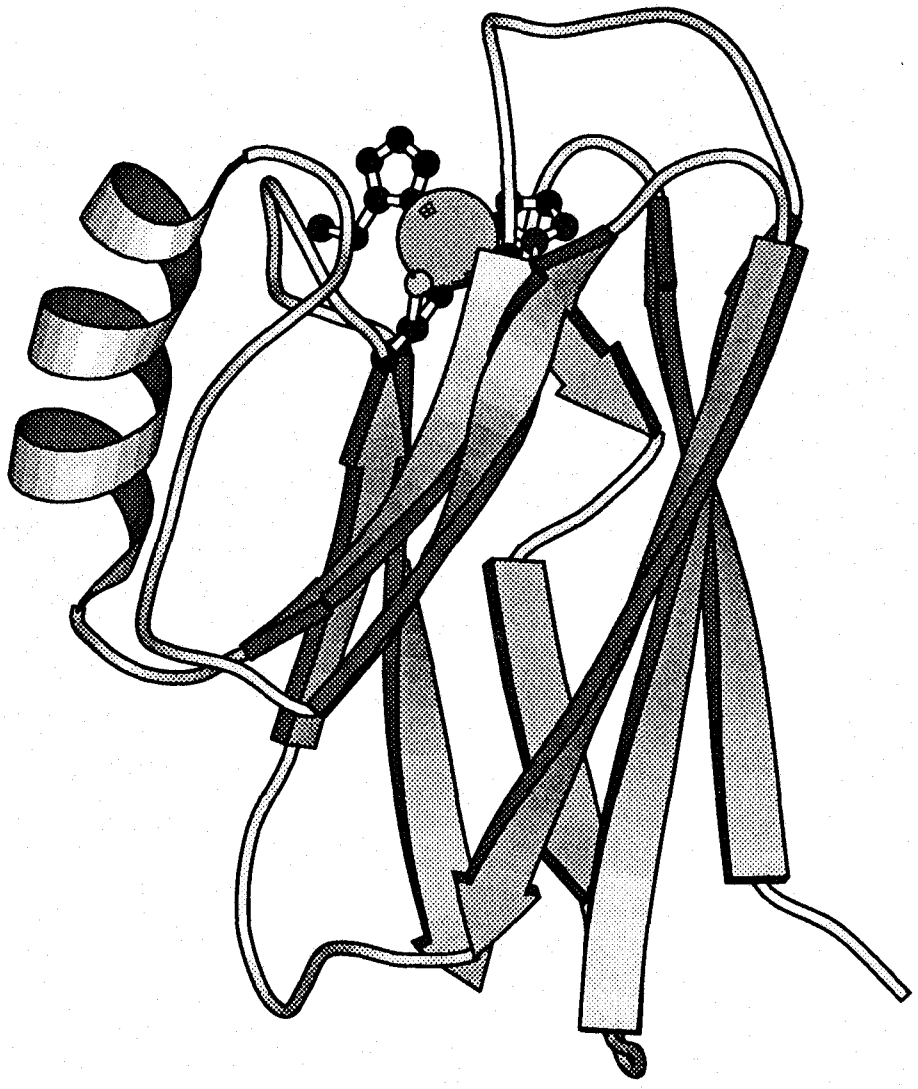

Fig. 4-5 (c) Schematic drawing of AZUNCIB

plastocyanin molecules. The location of the copper atom is the northern end of the molecule and the four ligand amino acids are also conserved. As will seen later, althogh, the topological diagram of azurin is different from that of pseudoazurin or that of plastocyainin.

Fig. 4-6 shows the superimposed structures of AZUNCIB and AZUNCTC. The averaged r.m.s. deviation for the backbone structures was calculated only 0.81Å. The very similar structures of azurins are thought to be reflected by the high proportions of identical residues of 90/129 (70%).

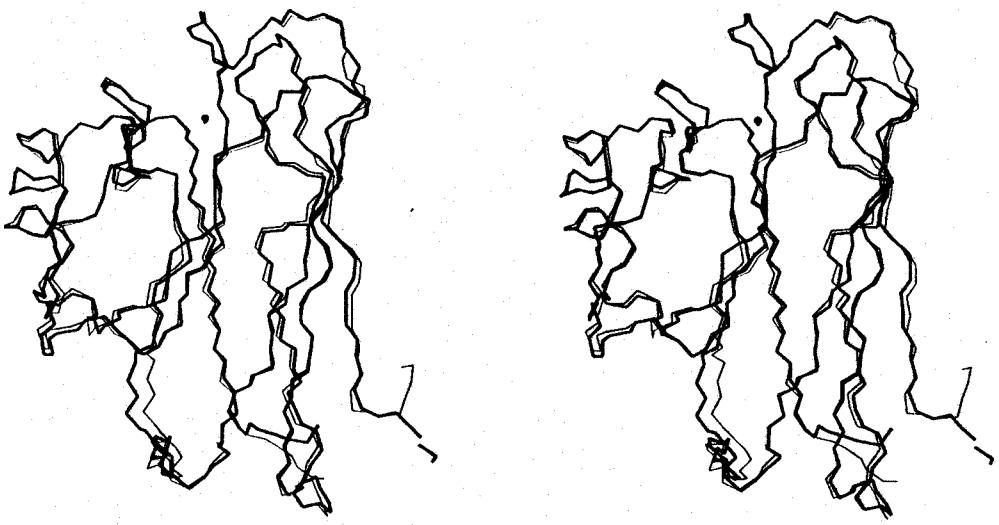

Fig. 4-6 A stereoview of the backbone structures of AZUNCIB and AZUNCTC superimposed. The thick lines show AZUNCIB and the thin lines show AZUNCTC. The r.m.s. error is only 0.81Å.

4-3 Comparison of the Molecular Structures among the Blue Copper Proteins

The whole structural features found in the obtained structures are common to those had been accepted in the blue copper proteins such as plastocyanin (Guss & Freeman, 1992), azurin (Baker, 1988), and amicyanin (Chen *et al.*, 1993). Although the amino acid sequences are considerably different from other blue copper proteins, it is very interesting that the topologies are quite similar (Fig. 4-7). It is common to all blue copper proteins that the active sites lie at the top of the molecules and four ligands of the metal are all conserved except stellacycnin. In all structures one histidine ligand commonly project from the molecular surface above the copper atom.

On the other hand, when the schematic drawings and the topological diagrams of three typical blue copper proteins are compared, some differences are found. While the plastocyanin molecules have no α–helix, the azurin and pseudoazurin molecules have one or two α–helixes. While the pseudoazurin molecules have two α–helixes at the C-terminal end, the azurin molecules have a α–helix between the strand IV and V. Four ligand residues are conserved in all blue copper proteins except stellacyain, but the arrangement of the residues is different. In the structure of

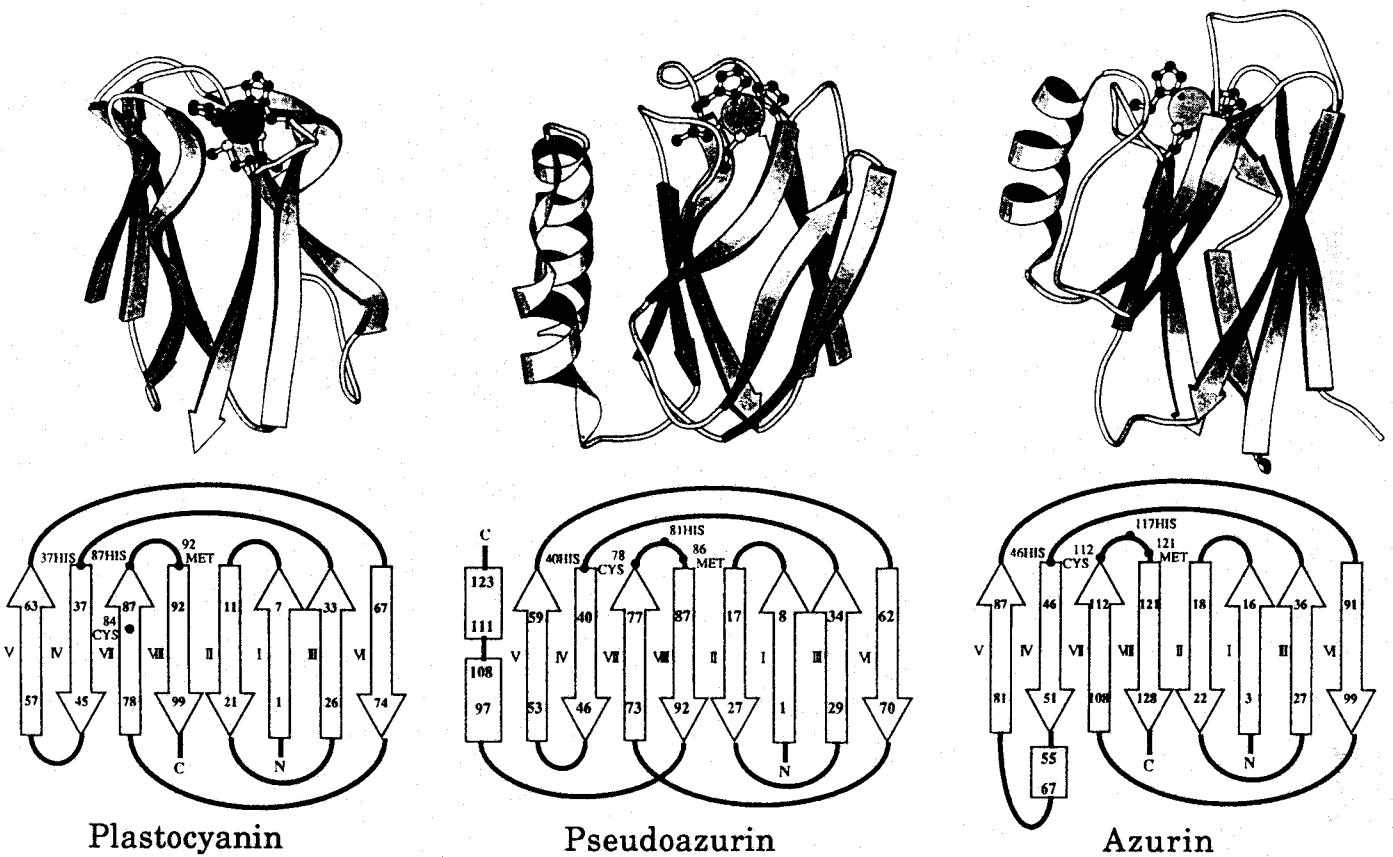

Fig. 4-7 Comparison of the overall structures and the topological diagrams among three typical blue copper proteins. Arrow show a β-strand and squares show an α-helix.

plastocyanin four ligands locate in the strand, but in ohter blue copper proteins some ligands locate in the loop. There are some differences concerning the molecular structures among the blue copper proteins, although, the whole structural features of them are generally common.

4-4 Copper Site of the blue copper proteins

All of the copper atoms are located near the top surface of the molecules (Fig. 4-7). However, it is common that one of the four copper ligands (His81) is projecting from the molecular surface above the copper atom. The distance between the copper atom and the molecular surface is about 6Å. In every blue copper protein, four ligands locating in the middle of two β–sheets surround the active site of the copper atom. In PAZAM1, one of the ligands (His40) is contained in the strand IV, but the others (Cys78, His81 and Met86) are located in the loop region which exists between the strands VII and VIII. In contrast, in plastocyanin the cysteine ligand is contained in the strand VII. Although the location of four ligands is different, these four amino acid residues are all conserved in the blue copper proteins except stellacyanin.

4-5 Copper Coordinations

4-5-1 Copper Coordinations of the Obtained Structures

Figs. 4-8 (a) and (b) show the electron density maps of PAZAM1 with the coefficient of $2F_O$-F_C around the copper atom calculated at 1.5Å resolution. Four ligand amino acids (His40, Cys78, His81 and Met86) are confirmed in the electron density and they are clearly connected with the large center circle of electron density of the copper ion. From these maps the coordination parameters of the copper atom could be calculated. The distances among the copper atom and four ligands in PAZAM1 are 2.07Å for Nδ1(His40)-Cu, 2.14Å for Sγ(Cys78)-Cu, 1.98Å for Nδ1(His81)-Cu, 2.65Å for Sγ(Met86)-Cu and 4.03Å for Oγ(Gly39)-Cu, respectively. The angle parameters among the copper atom and these ligands in PAZAM1 extend from the minimum of 86° to the maximum of 144°. From these structural parameters the geometry of the copper atom in PAZAM1 is also confirmed to be the distorted tetrahedral structure like PAZS6.

Meanwhile, from the electron density maps of PAZIAM calculated at 1.8Å resolution the distance parameters are 1.94Å for Nδ1(His40)-Cu, 2.17Å for Sγ(Cys78)-Cu, 2.10Å for Nδ1(His81)-Cu, 2.61Å for Sγ,(Met86)-Cu and 3.96Å for Oγ(Gly39)-Cu, respectively.

(a)

Fig. 4-8 Electron density map calculated at 1.5Å resolution around the copper atom in pseudoazurin. (a) The geometry of the copper atom is clearly a distorted tetrahedral structure formed by four ligands (His40, Cys78, His81 and Met86).

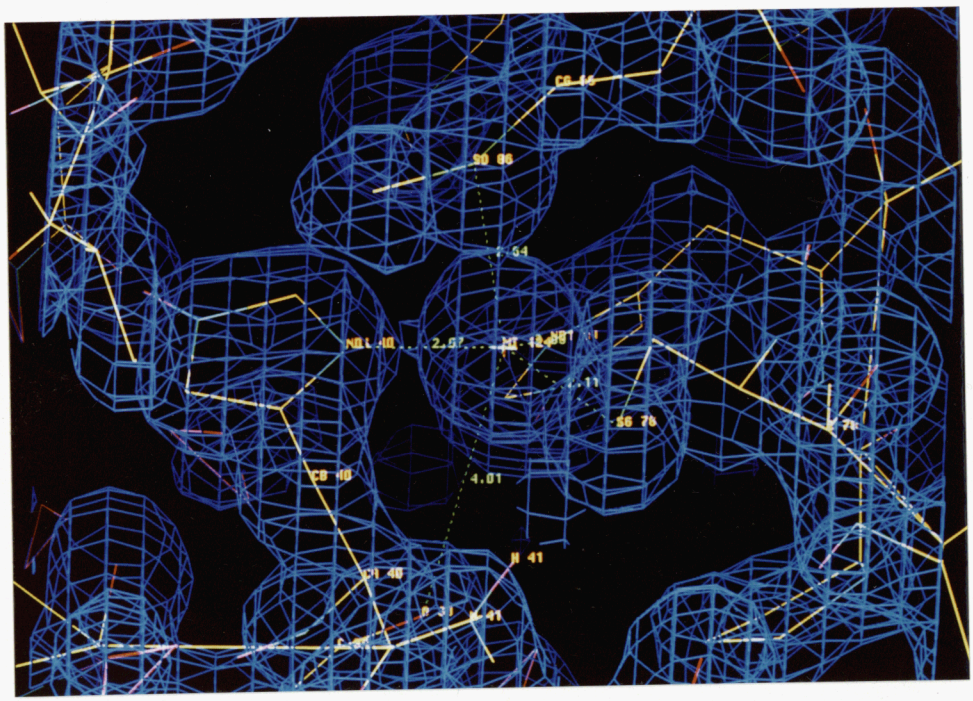

(b)

And Fig. 4-8 (b) shows the ligand Cys78 is bent from the tetrahedral structure by the conserved NH-S hydrogen bond.

The angle parameters as well as the distance parameters are similar to those of PAZS6 and PAZAM1.

Concerning the distance and angle parameters of AZUNCIB there are some errors resulted from the low resolution data. The coordination parameters was not listed, but, the active site structure of AZUNCIB was made clear as a distorted trigonal bypyramidal structure like AZUNCTC.

4-5-2 Comparison of the Copper Coordination Geometries

The similar properties in all blue copper proteins such as absorption and EPR spectrum are thought to be brought by the four conserved ligands of the copper atom. The slight difference of these properties may be resulted from the small deformations of the coordination geometries around the copper atom. Table 4-2 and Fig. 4-9 shows the comparison of the copper coordinations with typical blue copper proteins. In order to obtain and compare the precise parameters of the copper geometry, the structures revealed at atomic resolution were used to calculate. They containe three pseudoazurins; one is pseudoazurin from *Alcaligenes faecalis* S-6, another is pseudoazurin from *Methylobacterium extorquens* AM1, the other is *Achromobacter cycloclastes* IAM1013. And other two blue copper proteins which is analysed at high resolution are also

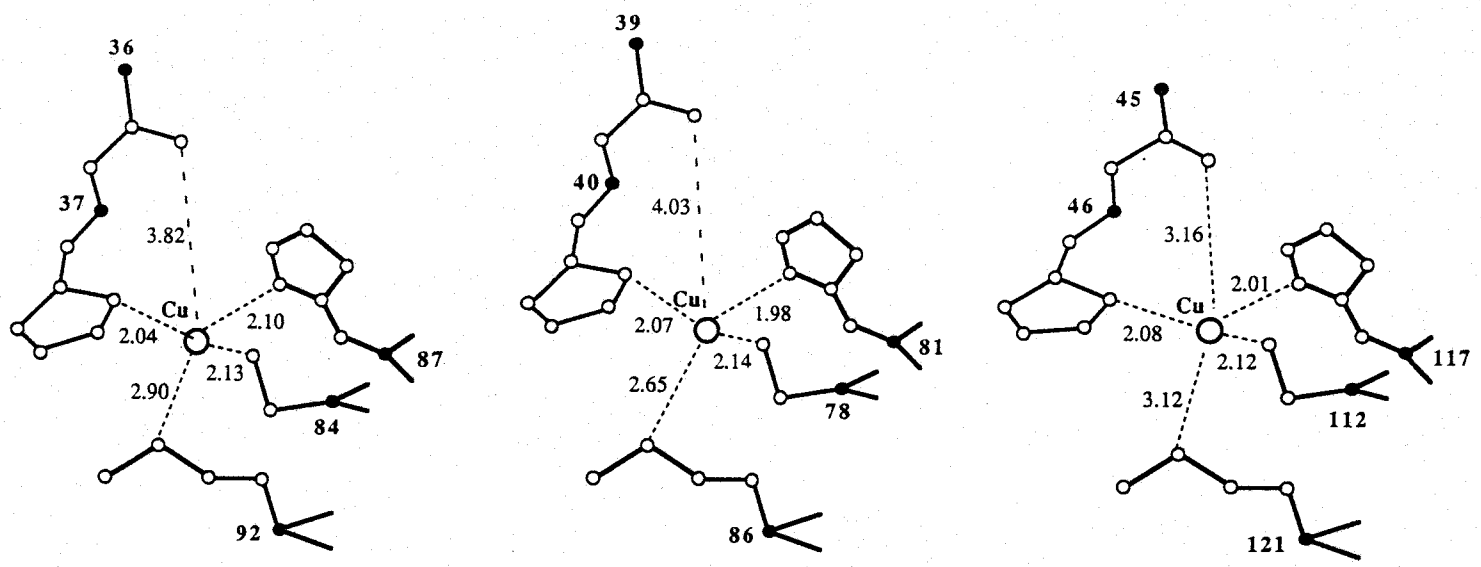

(a) Plastocyanin (b) Pseudoazurin (c) Azurin

Fig. 4-9 Comparison of the metal site structures among the typical blue copper proteins; a) plastocyanin from *poplar*, b) PAZAM1 and c) AZUNCTC.

Table. 4-2 *The geometry around the metal in some typical blue copper proteins*

Distance Parameter (Å)

	Nδ of His (1)	Sγ of Cys (2)	Nδ of His (3)	Sγ of Met (4)	Oxygen atom
PAZAM1*	2.07	2.15	1.97	2.66	4.03
PAZS6†	2.20	2.14	2.27	2.67	3.99
PCY‡	2.04	2.13	2.10	2.90	3.82
AZA§	2.08	2.12	2.01	3.12	3.16

Angle Parameter (Å)

	1-Cu-2	1-Cu-3	1-Cu-4	2-Cu-3	2-Cu-4	3-Cu-4
PAZAM1*	143.8	93.8	85.8	110.1	108.6	111.8
PAZS6†	138.4	100.0	86.3	111.7	107.0	108.8
PCY‡	132.1	96.6	85.4	122.9	108.1	102.7
AZA§	135.3	100.9	78.8	121.6	109.5	93.5

* Pseudoazurin from *Methylobactrerium extorquens* AM1 ‡ Plastocyanin from *poplar leaf*

† Pseudoazurin from *Alcaligenes faecalis* S-6 § Azurin from *Alcaligenes denitrificans* NCTC8582

contained. One is azurin from *Alcaligenes denitrificans* NCTC8582 and the other is plastocyanin from *poplar leaf*. Because the structure of AZUNCIB was obtained at 2.5Å resolution and the structure of AZUNCTC was reported at 1.8Å resolution, the atomic coordinates of AZUNCTC from the BNL protein data bank were used to obtain more precise parameters. As for plastocyanin the atomic coordination of *poplar*, which is analysed at 1.6Å resolution, was used to calculate the coordination parameters. The copper coordination parameters of the typical blue copper proteins are summarized in Table 4-2. The table shows three strong interactions and two weak interactions for each copper ion and there is a large difference of the copper geometry among these typical blue copper proteins.

In the structure of AZUNCTC the distance of Sγ(Met121)-Cu elongates to 3.12Å, while the oxygen atom of glycine approaches to the copper atom up to 3.16Å. These two atoms locate on both sides of the base plane formed by three other ligands containing two histidines and a cystein. The copper coordination in AZUNCTC was reported as the distorted trigonal bypyramidal structure (Baker, 1988). This coordination geometry of copper atom is also confirmed in the structure of azurin from *Achromobacter xylosoxidans* NCIB11015 (Inoue *et al.*, 1994). In PAZAM1, however, the oxygen atom of Gly39 is located 4.03Å from the copper atom and the interaction of the

glycine with copper atom is disappeared like in the structure of PAZS6 and PAZIAM. The metal coordinations of three pseudoazurins, PAZAM1, PAZIAM and PAZS6, are the distorted tetrahedron. In the structure of poplar plastocyanin the carbonyl oxygen of proline corresponding glycine in pseudoazurins and the Sγ atom of methionine locate at the distance of 3.82Å and 2.90Å from the copper atom, respectively. Since the carbonyl oxygen of proline may be free from the interaction with the copper atom, plastocyanin has also the distorted tetrahedral structure like pseudoazurins.

The geometrical differences around the copper atom among the typical blue copper proteins are also reflected in the positional deviations of the copper atoms from the base plane containing the δ-nitrogen atoms of two histidine ligands and the sulfur atom of cysteine ligand (Fig. 4-10). In the case of PAZAM1, the copper atom is deviated at 0.39Å from the plane toward the side of methionine. This value is very close to that of PAZIAM (0.43Å) or PAZS6 (0.38Å). On the other hand, for plastocyanin and azurin the corresponding distances are 0.34Å and 0.18Å, respectively. From these deviations as well as the copper coordination geometries, the metal site structures of pseudoazurins are found to be very close to that of plastocyanin rather than that of azurin.

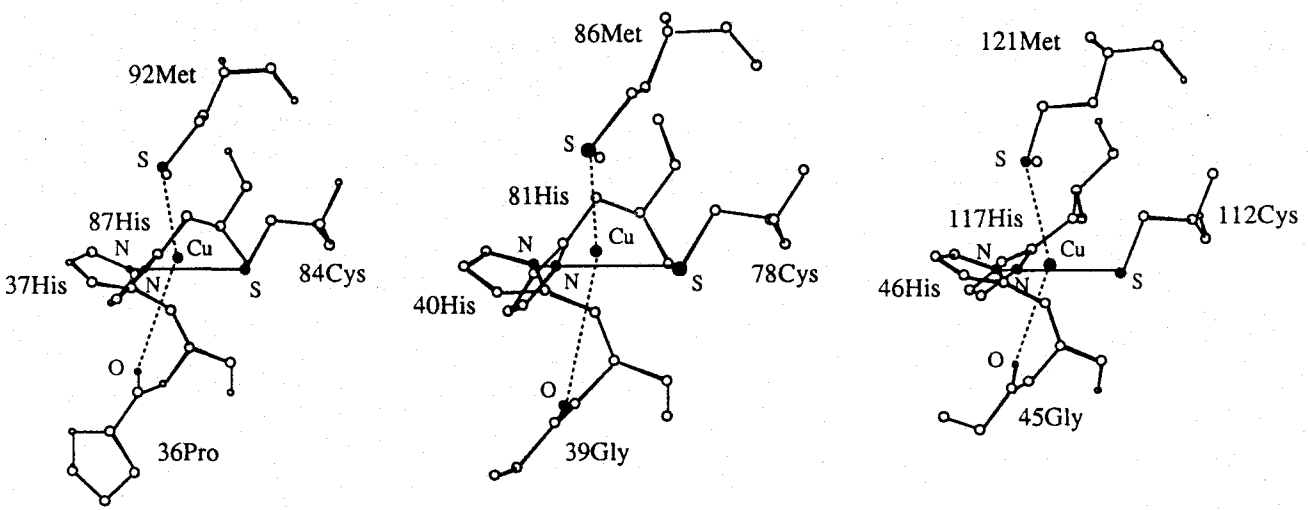

Plastocyanin **Pseudoazurin** **Azurin**

0.39Å 0.34Å 0.18Å

Fig. 4-10 Comparison of the copper deviations from the base plane that made by two ligand histidine and the ligand cysteine.

4-6 Interactions around the Ligand Atoms

4-6-1 Direct Interactions of the Hydrogen Bonding to the Ligand Atoms

The ligand conformations around the copper is possible to be affected by the various interactions with the neighboring groups within the copper coordination sphere such as amino residues or water molecules of crystallization. The interaction of the copper ligands with the amino residues includes two modes, one is the direct interaction with the ligand atom which cause the slight change of the orientation of the copper ligand and the other is the indirect interaction to modify the effect.

Concerning the direct interaction of neighboring groups with the copper ligands in PAZAM1, two amide protons of Asn41 and His81 are possible to hydrogen bond to the ligand sulfur atom of Cys78 in PAZAM1 as shown in Fig. 4-11. The N-S distances between Cys78 and Asn41 or His81 are 3.58Å and 3.67Å, respectively. The angles for hydrogen bonds are 103.2° for Cu-S-N(Asn41) and 93.8° for Cu-S-N(His81). From these parameters, the first hydrogen bond from the residue of Asn41 is fairly strong and may affect the orientation of the ligand cystein, while the second NH-S hydrogen bond from His81 is rather weak.

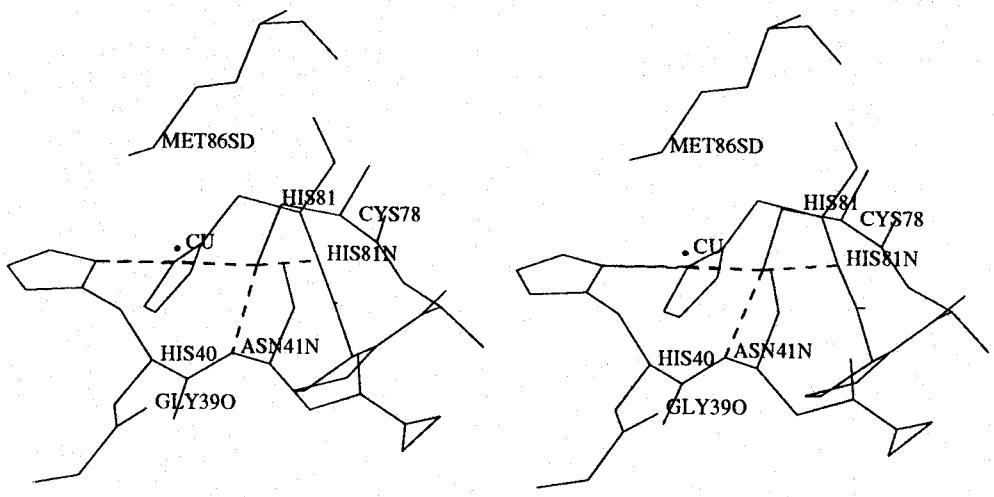

Fig. 4-11 Stereoview ot the metal site structure in PAZAM1. Two NH-S hydrogen bondings are observed between the the ligand cysteine and amido groups of Asn41 and His81.

In PAZIAM the N-S distances between Cys78 and Asn41 or His81 are 3.65Å and 3.98Å, respectively. Therefore, there is only one hydrogen bonding which from the amide proton of Asn41 to the sulfur atom of the ligand cysteine. The second hydrogen bond found in PAZAM1 is not occurred in PAZIAM, because of the long N-S distance.

Fig. 4-12 and Table 4-3 show the comparison of the mode of the conserved NH-S hydrogen bond in PAZAM1 with other typical blue copper proteins. In AZUNCTC two NH-S hydrogen bonds are formed between Asn47 or Phe114 and the sulfur atom of cystein ligand, the N-S distances are 3.52Å and 3.50Å, respectively. The angles of the Cu-S-N(amide nitrogen) are calculated as 103.8° for Asn47 and 115.4° for Phe114, respectively. Both of two amide nitrogens locate below the base plane and interact with the sulfur atom of cystein ligand from the underside of it. On the other hand, in the structures of PCY or three pseudoazurins the NH-S hydrogen bond between the cystein ligand and the conserved asparagine residues is fairly strong to fix the sulfur atom, but the second NH-S hydrogen bond to the amide group of the histidines don't interact to the sulfur atom (Table 4-3). As will be seen later in detail, the different number of the NH-S hydrogen bondings may be owing to the sequence homology in the loop region which contains three ligand

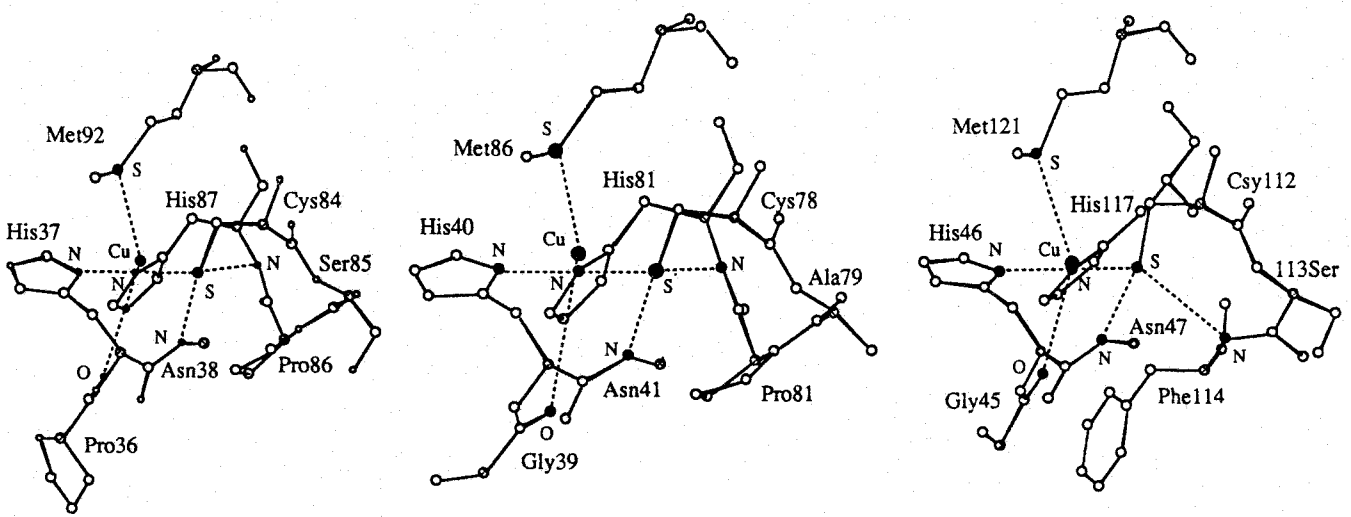

Fig. 4-12 Comparison of NH-S hydrogen bonding around the ligand cysteine among three typical blue copper proteins. While azurin has two NH-S bonding, pseudoazurin and plastocyanin have only one.

Table 4-3. *Comparison of the bond lengths and the angles of the NH-S hydrogen bonds around Cys78**

	Bond length		Angle parameters					
	S-N(1)	S-N(2)	Cu-S-C_β	Cu-S-N(1)	Cu-S-N(2)	C_β-S-N(1)	C_β-S-N(2)	N(1)-S-N(2)
PAZAM1	3.59	3.68	106.4	103.2	93.8	103.1	103.1	143.1
PAZS6	3.68	3.80	105.8	104.0	89.0	109.6	96.6	145.7
PCY	3.41	4.19	109.7	109.5	86.3	110.4	96.0	141.2
AZA	3.52	3.50	106.7	103.8	115.4	107.1	119.2	103.3

* In PAZ and PCY, N(1) and N(2) correspond to the amido group of the conserved Asn and His, respectively. In AZA, N(1) and N(2) correspond to that of the conserved His and Phe, respectively.

amino acid and the difference of the sequence homology in that region may dertermine the active site structure of whether distorted tetrahedral one or distorted trigonal bypyramidal one.

4-6-2 Indirect Interaction of the Hydrogen Bond to the Copper Geometry

Indirect interaction has also been reported between two histidine ligands through the hydrogen bonds including water-water bridge in both the X-ray structures of PAZS6 and PCY, but in AZA this type of water-water bridge was not found. In PAZAM1, the carbonyl oxygen of Asn9 is located at 2.70Å from the His40 $N_{\varepsilon 2}$ (Fig. 4-13). The Asn9 exists in the loop region between the β–strands I and II and is placed under constraint only by a water molecule (Water153) which locates at the distance of 2.66Å from Asn9. In order to form the water-water bridge between Asn9 and His81 water molecule 153 must interact with another water molecule around His81 $N_{\varepsilon 2}$. The electron density was, however, so weak that the second water molecule around the His81 $N_{\varepsilon 2}$ was not located in the electron density map. Thus, the hydrogen bond of Asn9 to His40 has little possibility to change the direction of the ligand histidines in PAZAM1.

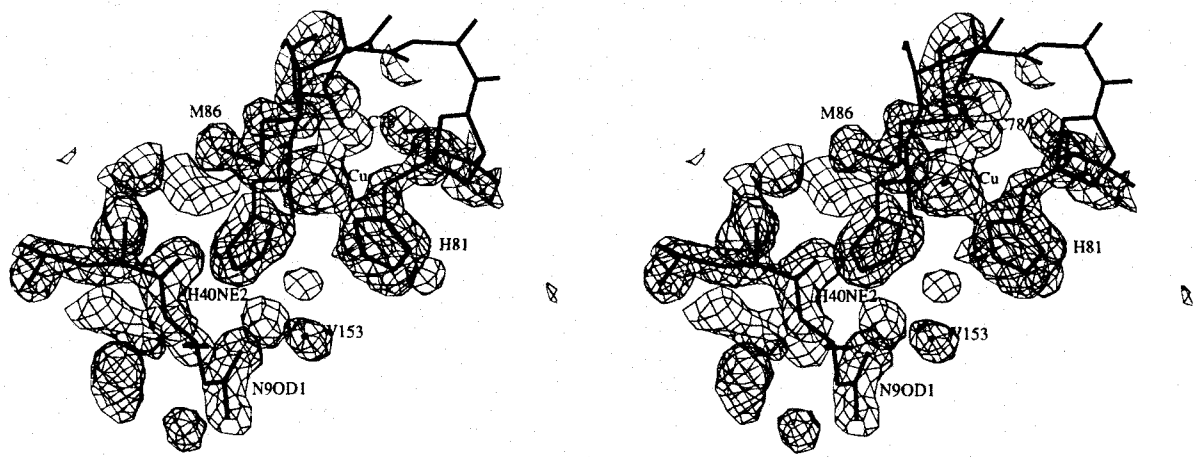

Fig. 4-13 Electron density map (*2Fo-Fc*) around the ligand His81 showing the hydrogen bond between $N_{\varepsilon}2$(His40) and $O_{\delta}1$(Asn9). This oxygen atom also hydrogen bonds to the Water153. In AZA and PCY this water molecule forms the water-water bridge between two ligand histidines.

The conserved Asn41 residue in PAZAM1 hydrogen bonds not only to the ligand sulfur atom of Cys78 but to the Ala79. The second hydrogen bond between Asn41 and Ala79 may indirectly affect the direction of the ligand sulfur atom of Cys78. Ala79 in PAZAM1 is replaced by threonine in another two pseudoazurins. In the structure of PAZS6 the hydrogen bond between Asn41 and Thr79 was reported to fix the loop containing three ligands to the β–strand IV. The effect of the replacement from alanine to threonine is, however, considered to be quite little since the visible spectrum of PAZAM1 and PAZS6 are quite similar to each other.

5 Correlation between the Metal Site Structures and the Properties

5-1 Correlation between Absorption Spectrum and the Structures

The name of the blue copper proteins is derived from their characteristic color, as described previously. The absorption spectrum around 600nm is from 50 to 100 times as strong as the normal copper complex. While the azurin have the maxmum absorption spectrum at 625nm, plastocyanin and pseudoazurin have at 597nm. It is reported that the large absorption band in the visible absorption range is caused by the charge transfer transitions from the sulfur atom of the cysteine ligand to the copper atom. Conserning the distance and angle parameters around the ligand cysteine there is no difference among three kinds of blue copper proteins (Fig. 5-1).

From the detailed structural comparisons among blue copper proteins, I consider the most significant reason for the subtle difference of the visible absorption is copper geometry. As observed in the structures of two pseudoazurins and plastocyanin, when the copper atom has a distorted tetrahedral structure, the protein would absorb at 600 nm, while if the copper atom has a distorted trigonal

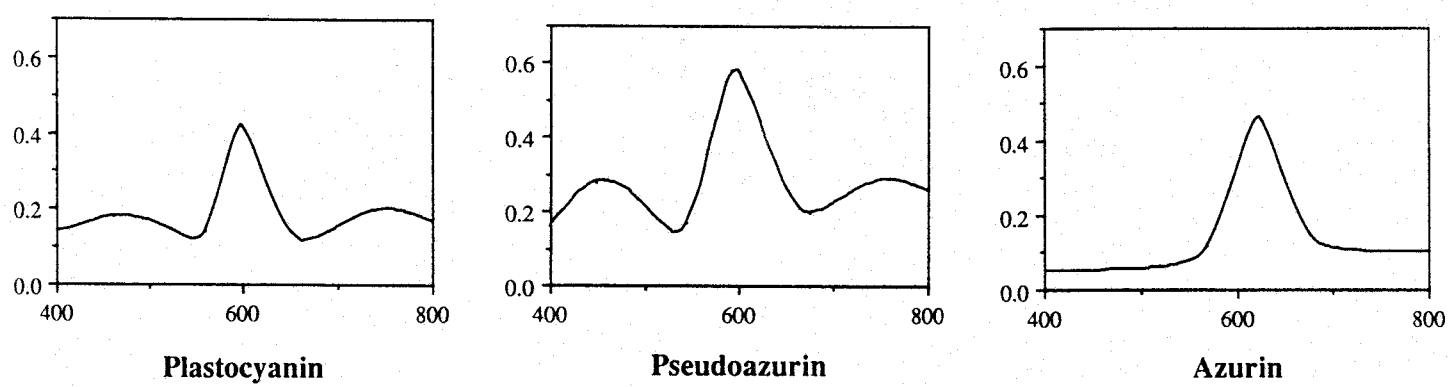

	N_{δ}(His)	S_{γ}(Cys)	N_{δ}(His)	S_{γ}(Met)	Oxygen atom	Abs. max(e)
Pseudoazurin	2.07	2.15	2.17	2.64	3.99	593 (3090)
Plastocyanin	2.04	2.13	2.10	2.90	3.82	597 (4900)
Azurin	2.08	2.12	2.01	3.12	3.16	625 (3500)

Fig. 5-1 Comparison of the visible absorption spectra and copper geometries among three blue copper proteins. While azurin have the maxmum absorption spectrum at 625 nm, others do at 600 nm. There is no answer in the distance parameters around the ligand

bypyramidal structure like AZUNCTC, the protein would absorb at 625nm. This is related to the fact that the fifth ligand of the oxygen atom of glycine or proline interact to the copper atom or not.

Baker and Adman suggested that the slight difference of the absorption curve between those of azurin and pseudoazurin or plastocyanin was resulted from the different number of the hydrogen bonds to affect the coordination geometry of copper atom or the electronic charge on Cys78 Sγ. Since both pseudoazurin and plastocyanin have only one NH-S hydrogen bond in contrast to the azurin of two, the modification of the absorption spectra may occur (Baker, 1988; Adman *et al.*, 1989).

I forcus on the differences of the metal site structures in the typical blue copper proteins in section 4. Consequently, it may be said that the blue copper proteins have a common NH-S hydrogen bonding from the conserved asparagine residue and the orientation of the ligand cysteine is distorted. Because the remarkable absorption band has to do with the charge transfer transitions from the ligand cysteine to the metal ion (CT-transition), the first NH-S hydrogen bond may enlarge the overlap of the electron-orbitals between the sulfur atom and the copper atom. It is delicate that whether the second NH-S hydrogen bond found in PAZAM1 significantly interact with the sulfur atom or not, but the geometrical

differences among three typical blue copper proteins may be occurred by the difference in the orientation of cysteine. The angle parameters of near 109° around two NH-S hydrogen bondings show the pπ-orbital of the sulfur atom easily orient to the $d_{x}2_{-y}2$ orbital of the copper atom. Therefore when the second NH-S hydrogen bonding is weak or nothing as in pseudoazurin or plastocyanin, the overlap between $d_{x}2_{-y}2$ orbital of copper atom and pπ-orbital of the cysteine sulfur atom decrease a little and the gap of the CT-transition is a little larger than that in azurin. The visible absorption may occur at 600 nm. In opposition that, azurin has the maximum absorption at 625 nm, because two NH-S hydrogen bondings increase the overlap of two orbitals.

Fig. 5-2 shows the comparison of the amino acid sequences from Tyr74 to Met86 in PAZAM1 together with the corresponding sequences in PCY and AZUNCTC. The amino acid of Phe114 in AZUNCTC is conserved in 9 kinds of azurin whose amino acid sequences have already been analysed, while in both pseudoazurin and plastocyanin there is no amino acid on the corresponding position of Phe114 in AZA. Asn41 in PAZAM1, which is next to the first histidine ligand, is conserved in all pseudoazurins, and the corresponding residue is also conserved in all blue copper proteins as Asn38 in plastocyanins and as Asn47 in azurins. These asparagine

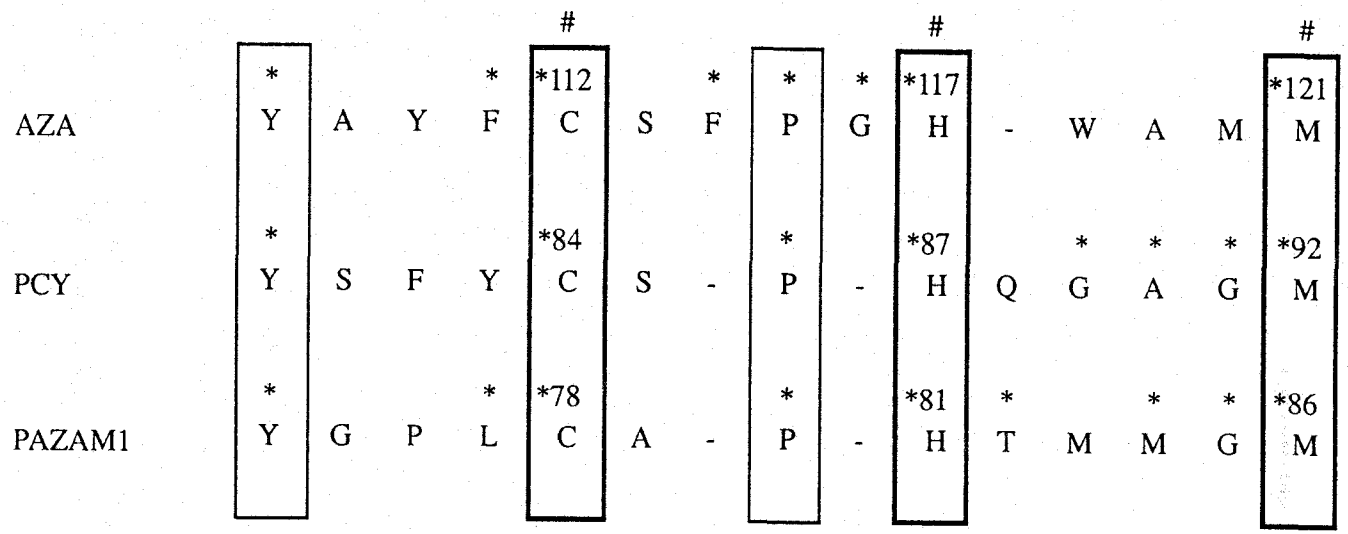

Fig. 5-2 Comparison of the amino acid sequences in the loop region near the copper atom. Three typical blue copper proteins (PAZAM1, AZUNCTC and PCY) are compared. # shows the ligand residue of the copper atom and * shows the conserved amino acid in the same kinds of the proteins.

residues commonly offer a hydrogen bond (NH-S) to the cysteine S atom from the downside of the base plane. A pair of histidine or phenylalanine and asparagine residues contained in a β–strand may be important to induce geometrical distortion in the copper geometry.

Namely, in the case of two excessive amino residues existing in the loop region between the strands VII and VIII in AZA two strong NH-S hydrogen bonds are formed under the base plane of the trigonal bypyramidal structure. On the other hand the lack of two amino residues and only existence of substitute amino acid of the conserved proline may change the mode of the second NH-S hydrogen bond to ligand cysteine and the tetrahedral structure is formed in PAZAM1 and PCY. These two copper geometry may reflect the different two kinds of the visible absorption spectrum.

The difference of EPR spectrum among the typical blue copper proteins is also explained by the same theory (Fig. 1-2). When the overlap between the $d_{x^2-y^2}$ orbital of the copper atom and the pπ-orbital of the cysteine sulfur atom increase by two NH-S hydrogen bondings, the unpaired electron would be delocalized and the EPR spectrum of azurin is azial. But, when the overlap decrease like pseudoazurin and plastocyanin, EPR spectrum of them are rhombic.

The formal redox potential of PAZIAM was estimated to be 259.1±0.2 mV vs NHE at 25°C (0.1 M phosphate, pH 7.0). This value

show the dependent character on pH. The unexpected negative redox potential, 237 mV vs NHE (pH 11.3) was observed and the pattern of EPR spectra also change from rhombic to axial. When the overlap between the $d_{X}2_{-y}2$ orbital of the copper atom and the pπ-orbital of the cysteine sulfur atom increase and EPR shows axial, the d-electrons would be a little satisfied by the pπ-electrons of the cysteine sulfur atom and the redox potential reasonablly show the negative shift. In the same way, the property of narrow hyper fine splitting of blue copper proteins is also explained by the overlap of two orbitals.

5-2 Protein-Protein Interaction

5-2-1 PAZAM1

Blue copper protein is a family of electron-transfer proteins having a single copper atom at the active site. Redox center in the protein is usually located beneath the protein surface with 5-10 Å depth (Adman, 1991) with four ligands of four amin-acid residues. Recent kinetic (Sykes, 1990; Christensen, 1993; Chapman,1984), and theoretical (Christensen, 1990; Lowery, 1993; Lowery, 1993) studies of blue copper protein indicate the two distince electron-tranfer pathways, adjacent (~6Å) site proceeding from the copper atom

through the surface exposed histidine residue located at hydrophobic patch and remote (~13Å) site via another amino-acid residue such as tyrosine (plastocyanin) (Guss & Freeman, 1992), phenylalanine (plastycyanin and azurin) (Baker, 1988) (Kyritsis, 1993), histidine (ascorbate oxidase, laccase, and nitrite reductase) (Messershmidt, 1989), or lysine (pseudoazurin) (Messershmidt, 1990) (Fenderson, 1991).

From the structural information of MADH and amicyanin complex, the active site of copper was surrounded by nine hydrophobic residues containing one histidine ligand. Pseudoazurin from *M. extorquens* AM1 also has the hydrophobic area around the copper active site. The interior of PAZAM1 is hydrophobic, while the surface is relatively polar. Especially the opposite side of the copper active center are mainly surrounded by positively charged residues (Fig. 5-3). The aromatic residues lies from the hydrophobic end to this negatively charged region. Among them the residue of Tyr82, the next residue of the ligand His81, locates at the surface of the protein. This residue was surrounded by some basic residues. This may be the reason why the recognition of the electron donor and the acceptor occurs by these two patches; one is the hydrophobic area around the ligand His81 exposing on the molecular surface and the other is the basic patch around the Tyr82. However, the electron

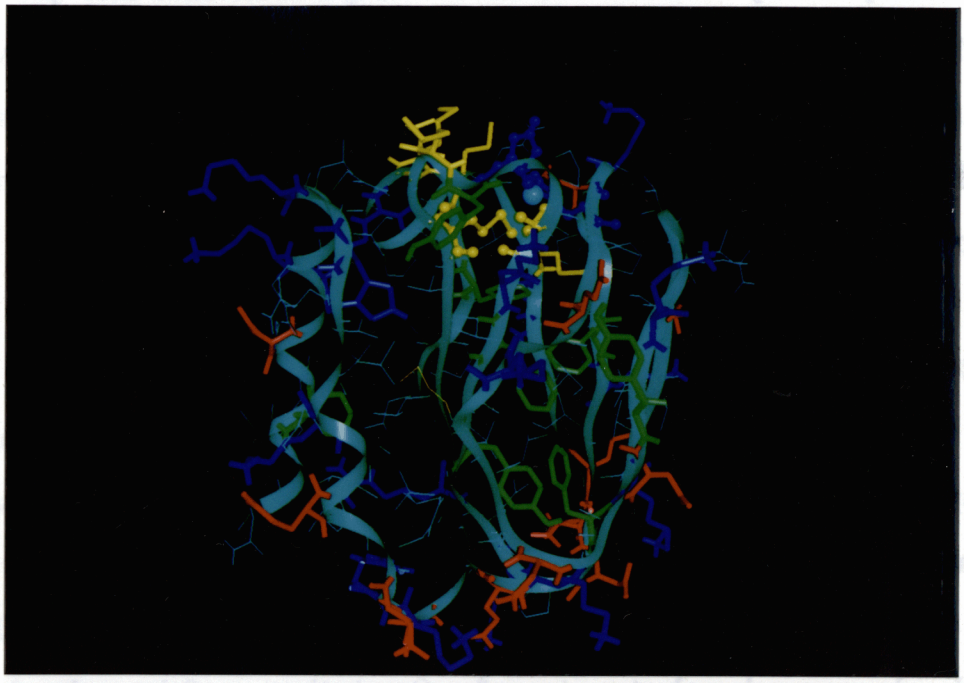

Fig. 5-3 Distribution of the amino acid residues in the structure of PAZAM1. Blue residues show the basic amino acids, red ones show the acidic amino acids and green ones show the aromatic amino acids, respectively. The copper atom is located at the top of the molecule (blue ball) and the hydrophobic patch consisted by mainly methionine (yellow residues) is formed around the copper atom. Hydrogen atoms are partially included based on the geometrical calculations.

transfer pathway in the bacterium of *Methylobacterium extorquens* AM1 has not been determined yet. It is a future problem to solve what is the pathway for electron transfer in blue copper protein as well as to see why pseudoazurin grows instead of amicyanin in the high concentration of copper in growth media.

5-2-2 PAZIAM

PAZIAM acts also as an electron-carrier in microorganism's respiration chain and is native electron-donors to the respective nitrite reductase.

Two sites have been identified on the surface of the PAZIAM molecule concerning electron transfer. One is the top of the molecular surface containing His81, and the other is a remote site containing the Lys77 which is an adjacent residue of the ligand Cys78 (Kohzuma & Suzuki, 1994). The first region is the hydrophobic patch as in plastocyanin or amicyanin (Guss, 1992, Chen, 1988) and is able to interact with a positively charged redox couple, which is important electron-transfer pathway via His-81 (*adjacent site*). In contrast, the second region containing the exposed Lys-77 of *remote site* is surrounded by some basic residues, which are concentrated in upper site of the molecule. The *remote site* linked copper center via Cys-78 is presumably electron-transfer site of pseudoazurin with a

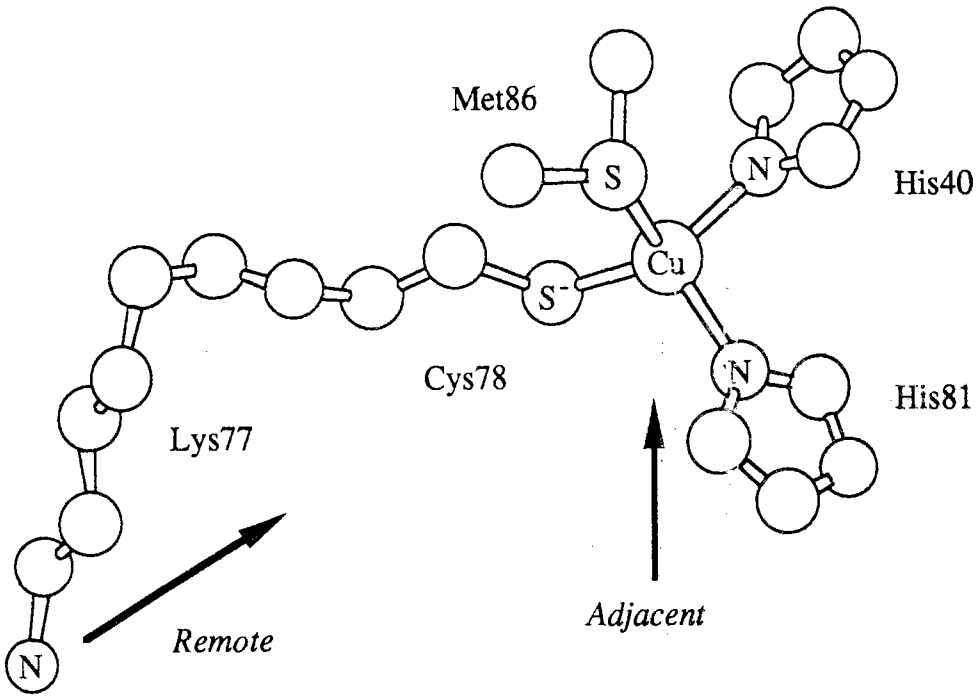

Fig. 5-4 Exposed lys-77 of *remote site* linked copper center via Cys-78 is presumably electron-transfer site of pseudoazurin with a negatively charged redox couple, NIR.

negatively charged redox couple (Fig. 5-4).

The electron transfer is reported to be carried out from a pseudoazurin to a nitrite reductase and the binally complex (1:1) is also confirmed. The detail of the electron tarnsfer chain may be able to be made clear by the X-ray crystallographic study of the complex with the nitrite reductase. From this standpoint the preliminally crystallographic studiy of the complex is in progress.

6 Conclusion

Blue copper proteins is a family of electron-transfer proteins having a single copper atom at the active site, which shows intense absorption band due to CT charge-transfer and irregularly narrow hyperfine splitting in the EPR spectrum. In order to make clear the relationships between the three-dimensional structures and their characteristic functions in the blue copper proteins and to establish the structural principle for synthesizing a copper complex with the characteristic functions in the blue copper proteins, I tried X-ray crystallographic studies on four blue copper proteins. I have succeeded in analyzing three molecular structures of blue copper proteins by molecular replacement method and three molecular structures have been obtained relatively at high resolution. One is pseudoazurin from *methylobacterium extorquens* AM1 analyzed at 1.5Å resolution, another is pseudoazurin from *achromobacter cycloclastes* IAM1013 at 1.8Å resolution, the other is azurin from *achromobacrer xylosoxidans* NCIB11015 at 2.5Å resolution. One of them, PAZAM1 was analyzed by molecular replacement combined with MAD method. Data collection near the absorption edge of the metal which is contained in the metalloprotein and easy calculations could offer the metal location that was very useful for the calculation

of MR method. Because every metalloprotein contains some inherent metal ions in its molecule, MAD method is very useful. The more convenient to utilize synchrotron radiation is and the more the number of the three-dimensional structure in PDB is, the more important for metalloproteins to collect the anomalous data from now on.

The comparison among the structures of typical blue copper proteins revealed that the active site structures of them are devided in two, one is distorted tetrahedral structures and the other is distorted trigonal bypyramidal structure, in opposition to the resembleness of the overall structures. Two active site structures reflect the differences of the characteristic properties, such as visible absorbance, EPR spectrum and reduction potential. The detail comparisons made clear that the sole cause possible to change the structure of active site is the NH-S hydrogen bondings aroun the ligand cysteine. If there were two NH-S hydrogen bondings, the active site of structure would be distorted trigonal bypyramidal, and if there were only one, it would be a distorted tetrahedral structure. Moreover, it has also been made clear that the amino acid's conservation in the loop region, in which 3 ligand amino acids are contained, would concern directly with the number of NH-S hydrogen

bond. Therefore, the homology of the amino acid sequences in the loop region would determine the active site structures in conclusion.

The structural principle of the blue copper protein obtained in this work is thought to be as below. The electron charge transfer from the satisfied orbital of the soft ligand to the unsatisfied orbital of the metal center may produce the singular character through the overlap between $p\pi$-orbital and $d\pi$-orbital. This is why it is very available to introduce a certain interaction like NH-S hydrogen bonding, which bends the direction of the ligand in order to synthesize a small molecule with the characteristic property.

A little information about the functions as the electron-transfer are obtained by this work, although the details will be obtained by the X-ray crystallography of the complexes between the blue copper proteins and their redox couples.

References

Adman, E. T., Turley, S., Bramson, R., Petratos, K., Banner, D., Tsernoglou, D., Beppu, T., Watanabe, H. (1989). *J. Biol. Chem.* **264**, 87-99.

Adman, E. T., Stenkamp, R. E., Sieker, L. C. and Jensen, L. H. (1978) *J. Mol. Biol.* **123**, 35-47

Adman, E. T. (1991) *Advances Protein Chemistry* **42**, 145-197.

Ambler., R. P., & Tobari, J. (1985). *Biochem. J.* **232**, 451-457.

Ambler, R. P. (1977). *The Evolution of Metaloenzymes, Metalloproteins and Relate Materials*, edited by G. J. Leigh, pp.100-118. London: Symposium Press.

Baker, E. N. (1988). *J. Mol. Biol.* **203**, 1071-1095.

Brünger, A. T., Kurian, J. & Karplus, M. (1987). *Science.* **235**, 458-460.

Brünger, A. T., Krukowski, A. & Erickson, J. W. (1989). *Acta Cryst.* **A46**, 585-593.

Chen, L., Mathews, F. S., Davidson, V. L., Tgoni, M., Rivetti, C. & Rossi, G. (1993) *Protein Science,* **2**, 147-154.

Chen, L., Louis, W. L., Mathews, F. S., Davidson, V. L., & Husain, M. (1988). *J. Mol. Biol.* **203**, 1137-1138.

Chapman, S. K., Knox, C. V. and Sykes, A. G. (1984) *J. Chem. Soc.*

Dalton Trans., 2775-2780.

Christensen, H. E. M., Conrad, L. S. and Ulstrup, J. (1993) *J. Arch. Biochem. Biophys.* **301**, 385-390.

Christensen, H. E. M., Conrad, L. S., Mikkelsen, K. V., Nielsen, M. K. and Ulstrup, J. (1990) *J. Inor. Chem.* **29**, 2808-2816.

Colman, P. M., Freeman, H. C., Guss, J. M., Murata, M., Norris, V. A., Ramshaw, J. A. M. and Venkatappa, M. P. (1978) *Nature* **272**, 319-324.

Crowther, R. A. (1972).*The Molecular Replacement Method*, edited by M. G. Rossmann, pp. 173-185. New york: Gordon and Breach.

Fenderson, F. F., Kumar, S., Adman, E. T., Liu, M. Y., Payne, W. J. and LeGall, J. (1991) *J. Biochemistry*,**30**, 7180-7185.

Ferrin, T. E. (1988). *J. Mol. Graphics* **6**, 13-27.

Fitzgerald, P. M. D. (1988). *J. Appl. Cryst.* **21**, 273-278.

Godden, J. W., Turley, S., Turley, S., Teller, D. C., Adman, E. T., Lie, M. Y., Payne, W. J. & LeGall, J. (1991) *Science*, **253**, 438-442.

Guss, J. M., Bartunik, H. D. and Freeman, H. C. (1992) *Acta Cryst.* **B48**, 790-811.

Hendrickson, W. A. & Konnert, J. H. (1981). *Biomolecular*

Structure, Function, Conformation and Evolution edited by R. Srinivasan, **1**, pp. 43-57. Oxford: Perganon Press.

Higashi, T. (1989). *J. Appl. Cryst.* **22**, 9-18.

Homel, S., Adman, E. T., Walsh, K. A., Beppu, T. & Titani, K. (1986).*FEBS Lett.* **197**, 301-304.

Inoue, T., Kai, Y., Harada, S., Kasai, N., Suzuki, S., Kohzuma, T. & Tobari, J. (1991). *J. Mol. Biol.* **218**, 19-20.

Inoue, T., Nakanishi, H., Koyama, S., Kai, Y., Harada, S., Kasai, N., Ohshiro, Y., Suzuki, S., Kohzuma, T., Iwasaki, H. & Shidara, S. (1994). in preparation.

Iwasaki, H & Matsubara, T. (1972) *J. Biochem.* **71**, 645-662.

Iwasaki, H., Noji, S. & Shidara, S. (1975) *J. Biochem.* **78**, 335-361

Jones, T. A. (1978). *J. Appl. Cryst.* **11**, 268-272.

Kohzuma, T., Sykes, A. G., Christopher, D., Nakashima, S., Kitagawa, T., Inoue, T., Kai, Y., Nishio, N., Shidara, S. & Suzuki, S. (1994) *to be submitted.*

Kyritsis, P., Messershmidt, A., Huber, R., Salmon, G. A. & Sykes, A. G. (1993) J Am. Chem, Soc. Dalton Trans., 731-735.

Lowery, M. D., Guckert, J. A., Gebhard, M. S. and Solomon, E. I. (1993) *J. Am. Chem. Soc.*, **115**, 3012-3013

Luzzati, V. (1952). *Acta Cryst.* **5**, 802-810.

Matthews, B. W. (1968). *J. Mol. Biol.* **33**, 491-497.

Messershmidt, A, Rossi, A, Ladenstein, R, Huber, R., Bolognesi, M., Gatti, G, Marchesini, A, Petruzzelli, R. & Finazzi-Agro, A. (1989) *J. Mol. Biol.* **206**, 513-529.

Messershmidt, A. & Huber, R. (1990) *J. Biochem.* **187**, 341-352.

Miyahara, J., Takahashi, K., Amemiya, Y., Kamiya, N. & Satow, Y. (1986). *Nuclear Instruments and Methods in Physics Research*, **A246**, 572.

Norris, G. E., Anderson, B. F., Baker, E. N. & Rumball, S. V. (1979), *J. Mol. Biol.* **135**, 309-312

Sakabe, N. (1983). *J. Appl. Cryst.* **16**, 542-547.

Sakabe, N. (1991). *Nuclear Instruments and Methods in Physics Research*, **A303**, 448-463.

Smeekens, S., Groot, M., Binsbergen, V. J. & Weisbeek, P. J. (1985) *Nature* **317**, 456-458.

Solomon, E. I., Lowery, M. D. (1993). *Science*, **259**, 1575-1581.

Steigemann, W. (1974). PhD thesis, Tecnishce Univ. München, Germany.

Strahs, G. (1969), *Science* **165**, 60-61.

Sykes, A. G. (1990). *Structure and Bonding* **75**, 175-224.

Thaller, C., Eichele, G., Weaver, L. H., Wilson, E., arlson, R. & Jansonius, J. N. (1985). *Methods in Enzymology* edited by Wyckoff, H. W., Hirs, C. H. & Timasheff, S. N., **114**

pp. 132-135. Academic Press, Inc. (London) LTD.

Turley, S., Adman, E. T., Sieker, L. C., Lie, M.-Y., Payne, W. J. and LeGall, J. (1988). *J. Mol. Biol.* **200**, 417-419.

Tobari, J. (1984). *Microbial Growth on C1 Compounds* edited by R. L. Crawford & R. S. Hanson, pp. 106-112, Washington: American Society for Microbiology.

Ward, K. B., Wishner, B. C., Lattman, E. E. & Love, W. E. (1975). *J. M. Biol.* **98**, 161-177.Reference

List of Publication

(1) Preliminary Crystallographic Study of a Pseudoazurin from Methylotrophic Bacterium, *Methylobacterium extorquens* AM1

T. Inoue, Y. Kai, S. Harada, N. Kasai, S. Suzuki, T. Kohzuma and J. Tobari

J. Mol. Biol., 1991, **218**, 19-20

(2) Crystallization and Preliminary X-Ray Studies on Pseudoazurin from *Achromobacter cycloclastes* IAM1013

T. Inoue, N. Nishio, Y. Kai, S. Harada, Y. Ohshiro, S. Suzuki, T. Kohzuma, S. Shidara and H. Iwasaki

J. Biochem., 1993, **114**, 761-762

(3) Refined Crystal Structure of Pseudoazurin from *Methylobacterium extorquens* AM1 at 1.5Å Resolution

T. Inoue, Y. Kai, S. Harada, N. Kasai, Y. Ohshiro, S. Suzuki, T. Kohzuma and J. Tobari

Acta Cryst. Section D, 1994, in press.

(4) Three-Dimensional Structure of Azurin from *Achromobacter*

xylosoxidans NCIB11015 at 2.5Å Resolution

T. Inoue, H. Nakanishi, S. Koyama, Y. Kai, S. Harada, N. Kasai, Y. Ohshiro, S. Suzuki, T. Kohzuma, S. Shidara, & H. Iwasaki

in preparation.

(5) Crystal Structure of Pseudoazurin from *Achromobacter cycloclastes* IAM1013 at 1.8Å Resolution

T. Inoue, N. Nishio, Y. Kai, S. Harada, Y. Ohshiro, S. Suzuki, T. Kohzuma, S. Shidara and H. Iwasaki

in preparation.

Supplementary Paper

(1) C-4 and C-5 Adducts of Cofactor PQQ (Pyrroloquinolinequinone). Model Studies Directed Toward the Action of Quinoprotein Methanol Dehydrogenase.
S. Itoh, M. Ogino, Y. Fukui, H. Murao, M. Komatsu, Y. Ohshiro, T. Inoue, Y. Kai and N. Kasai
J. Am. Chem. Soc., 1993, **115**, 9960-9967

Acknowledgment

The author wishes to express his sincerest gratitude to Professor Yoshiki Ohshiro for his precise suggestions and encouragement throughout this investigation.

The author is deeply indebted to Professor Nobutami Kasai for his helpful suggestions, his useful discussions and his hearty encouragement

The author wishes to make a grateful acknowledgment to Professor Yasushi Kai for his incessant and substantial guidance and his stimulating discussions throughout this investigation.

The author is deeply thankful to Dr. Shigeharu Harada for his useful discussions and advice of this work. Further, the author is deeply grateful to Dr. Kunio Miki, Dr. Nobuko Kanehisa for their kind guidance of X-ray structural study and their encouragement.

The author is deeply thankful to Professor Shinnichiro Suzuki and Dr. Takamitsu Kohzuma for their guidance and advice of the purification as well as their stimulating discussions.

The author is also grateful to Professor Y. Katsube of the Crystallographic Research Center, Institute for Protein Research, Osaka University, for the use of its facilities.

The author is also grateful to Professor N. Sakabe and Dr. A. Nakagawa of the National Laboratory for High Energy Physics (KEK) for the technical support during the data collection and their helpful discussions for MAD method.

And the author also thanks to Professor K. Hirotsu and Dr. A. Okamoto of Osaka City University for the kind supply of the programs *PEAK* and *WATER*.

Grateful acknowledgment are given to Mr. Hisao Nakanishi, Mr. Susumu Yamasaki, Mr. Hidekazu Ishii, Mr. Satoshi Koyama, Mr. Naoki Shibata and Mr. Nobuya Nishio for their collaboration in this work. Further, the author would like to thank all other members of in his laboratory for their kind assistance.

Finally, the author wishes to express his deep tanks to his parents for their perpetual assistance and encouragement.